SLAC-PUB-3129
May 1983
(T/E)

RADIATIVE CORRECTIONS TO e^+e^- REACTIONS TO ALL ORDERS IN α USING THE RENORMALIZATION GROUP*

YUNG SU TSAI
Stanford Linear Accelerator Center
Stanford University, Stanford, California 94305

ABSTRACT

Renormalization group technique is used to improve the accuracy of the lowest order radiative corrections in QED. The exponentiation of infrared terms comes automatically. It also leads to exponentiation of the vertex functions. It predicts the existence of conversion of photons into pairs and the result agrees with the Kroll-Wada relation. Kinoshita-Lee-Nauenberg cancellation of mass singularities occurs to all order in α in leading log approximation in the final state if we sum over all the final states. Higher order corrections to the order α^3 asymmetry is shown to be small. The results are used to derive useful formulas for the radiative corrections to processes such as $e^+e^- \to \mu^+\mu^-$, $e^+e^- \to \mu^+\mu^-\gamma$, e^+e^- → hadron continuum, e^+e^- → very narrow resonance such as ψ, and e^+e^- → not very narrow resonance such as Z^o.

Submitted to Review of Modern Physics
and
Presented at the Asia Pacific Physics Conference
Singapore, June 12-18, 1983

---

* Work supported by the Department of Energy, contract DE-AC03-76SF00515.

TABLE OF CONTENTS

I. INTRODUCTION

The aims of this paper are two-fold: The first is to demonstrate how the renormalization group technique can be used to improve the perturbation theory calculation in quantum electrodynamics (QED) and the second is to actually use the technique to write useful radiative correction formulas for the e^+e^- colliding beam experiments. In QED only the charge renormalization is necessary because the mass renormalization and the wave function renormalization cancel each other ($Z_1 = Z_2$). The renormalization group technique in QED is based on a very simple principle: "physics" should be independent of the value of photon invariant momentum λ^2 at which we renormalize the charge. That such a simple and seemingly obvious principle can lead to interesting physical consequences was first noted by Stueckelberg and Peterman (Stueckelberg, 1953), Gell-Mann and Low (Gell-Mann, 1954). In this paper we adopt the method developed by Bogoliubov and Shirkov (Bogoliubov, 1959). Eriksson (Eriksson, 1964,1968) was the first person to apply the renormalization group technique to QED radiative corrections. In this paper we improve upon Eriksson's treatments. In Appendix A we rederive Eriksson's results without using his assumption that the physical quantities such as vacuum polarizations, vertex functions, bremsstrahlung formula, cross sections etc. have well defined finite limits as $m \to 0$.

If one uses the renormalization group technique, all the masses in the problem are approximated by λ^2. This is a very bad approximation at presently available energies. For example at $(s)^{1/2} = 100$ GeV, we have $\ell n(s/m_e^2) = 24.4$, $\ell n(s/m_\mu^2) = 13.8$, and $\ell n(s/m_\tau^2) = 8.03$; therefore these quantities cannot be regarded as approximately equal for practical calculations. We must recover all the mass dependence from the results of the renormalization group technique in order to be of any use for practical applications. Especially in the application of the renormalization group technique to QED the vacuum polarization plays a very essential role and particles with all different masses occur here. Fortunately the result of the renormalization group is factorizable [see Eq. (2.15)] and each factor can be expanded in a certain way [see Eqs. (2.16) and (2.20)] so that its physical origin is manifest. Since we know the physical origin of each term, it is obvious what mass should be used in place of λ^2 in each part of the diagram. This problem of what masses to assign to each part of the Feynman diagrams can be solved automatically in one stroke if we replace the renormalization group result Eq.

(2.2) by Eq. (2.3). Thus our treatment is based on Eq. (2.3) throughout the rest of the paper. Since Eq. (2.3) reproduces completely the first order radiative corrections as well as all the leading log terms in the higher order corrections, the terms ignored are at most of order $\alpha^2 \ell n(q^2/m_e^2) \sim 0.14\%$ for $q^2 < (300\ \mathrm{GeV})^2$.

In Sec. II.A we write down the lowest order radiative corrections to the process $e^+e^- \to \mu^+\mu^-$ in the soft photon limit. This process was chosen because the results obtained here can be applied most easily to other processes. In Sec. II.B we use Eq. (2.3) to extend the results of the lowest order radiative corrections to all orders in α. The properties of the results of this extension are then discussed. The most important properties are:

1. The multiple photon exchange between different charged lines and the interference between the bremsstrahlung from different charged lines do not produce leading log terms in the cross section.
2. From the structure of Eq. (2.3), the result can be factorized into various parts, namely, the initial state vertex function, bremsstrahlung and pair conversion from the initial state, the vacuum polarization of the main photon propagator, the final state vertex function, the bremsstrahlung and pair conversion from the final state, and the corrections to the asymmetry. As mentioned earlier, because of this property of factorization, it is obvious what kind of mass to use in each part and our procedure gives this mass dependence correctly. The factorization is to be expected because we could have applied the renormalization group technique to each of these factors and obtained the same result.
3. The procedure produces the exponentiation of infrared terms automatically. It also tells us that the vertex function should be exponentiated but the vacuum polarization should not be. The latter should be summed into $(1 - \frac{1}{2}\delta_{vac})^{-1}$ instead.
4. It predicts the existence of pair conversion of a photon. This is remarkable since the starting point of the calculation (the lowest order radiative corrections) does not contain pair conversion of a photon. The result agrees with the Kroll-Wada (Kroll, 1952) relation between bremsstrahlung cross section and the internal pair conversion cross section.

5. Our results exhibit the cancellation of mass singularities discovered by Kinoshita (Kinoshita, 1961) and Lee-Nauenberg (Lee, 1963) to all order in α. This justifies that we do not do radiative corrections to the hadronic final states in the measurement of $R = \sigma(e^+e^- \to \text{hadrons})/\sigma(e^+e^- \to \mu^+\mu^-)$.
6. Higher order corrections to the asymmetry which was produced by the lowest order radiative correction are small.

In Sec. III we discuss how to do radiative corrections to process such as $e^+e^- \to \mu^+\mu^-\gamma$ which is itself not the lowest order cross section. In Sec. IV, we apply our result to the radiative corrections to $e^+e^- \to$ hadronic continuum. In Sec. V, we consider the radiative corrections to $e^+e^- \to$ narrow resonance $\to$ some final state where the width of the resonance is much narrower than the energy spread of the machine (such as in ψ). The procedure of extracting the full width, the leptonic width and other widths are discussed.

In Sec. VI, we consider the radiative corrections to $e^+e^- \to Z_0 \to f$, where Z_0 is supposed to have a width equal to or greater than 3 GeV which is much wider than the machine width. We investigate the effects of radiative correction to (1) shift in the peak positron; (2) reduction in the peak height; and (3) fattening of the full width at half maximum. Numerical examples using various width of Z_0 corresponding to different numbers of neutrino flavors are given. Sec. VII gives the concluding remarks.

II. SOFT PHOTON PART

Let us suppose that the *soft photon* part of the cross section including the radiative corrections to order α is given by

$$\sigma_1 = \sigma_0(1 + 2\Pi + A) \tag{2.1}$$

where σ_0 is the lowest order cross section, Π is the order α vacuum polarization and A is the rest of order α radiative corrections. Using the standard renormalization group technique we obtain in Appendix A the following expression for the radiative corrections to all order in α in the leading log approximation:

$$\frac{\sigma}{\sigma_0} = (1 + n.\ell.)\left(\frac{1}{1 - C_\pi\ \ell n\ q^2/\lambda^2}\right)^{(2C_\pi + C_A)/C_\pi} \tag{2.2}$$

where C_A and C_π are the coefficients of $\log q^2$ in A and Π respectively, and λ^2 is the value of q^2 at which the renormalization is carried out and it is assumed to be roughly the same order of magnitude as the masses of the particles involved, and $n.\ell.$ stands for the nonlogarithmic terms in $2\Pi + A$. Unfortunately the energy ranges of the colliding beam machines are not high enough for us to ignore the mass difference between m_e, m_μ, m_τ, m_u, m_d, m_c, m_b, etc. which can occur in the vacuum polarization Π in Eq. (2.1). Thus Eq. (2.2) will not give useful numerical results unless one can put back all the mass dependence which was lost in going from Eq. (2.1) to Eq. (2.2).

I propose that we replace (2.2) by the following formula:

$$\frac{\sigma}{\sigma_0} = \left(\frac{1}{1 - \Pi}\right)^{2+(A/\Pi)} \tag{2.3}$$

Before justifying the use of Eq. (2.3), let us write the expressions for Π and A using the radiative corrections to $e^+e^- \to \mu^+\mu^-$ as an example. We discuss later how our result should be modified to deal with the radiative corrections to $e^+e^- \to \mu^+\mu^-\gamma$, $e^+e^- \to$ hadrons (nonresonances), $e^+e^- \to$ resonance $\to f$ and $e^+e^- \to Z_0 \to f$.

A. Lowest Order Radiative Corrections to $e^+e^- \to \mu^+\mu^-$

For the reaction $e^+e^- \to \mu^+\mu^-$, the lowest order cross section is $d\sigma_0/d\Omega = (\alpha^2/4s)(1+\cos^2\theta)$ and the expressions for the Π and A in Eq. (2.1) are:

$$A = \delta_A + \delta^e_{vert} + \delta^\mu_{vert} - (t_e + t_\mu + t_{e\mu})\ \ell n\ \frac{E}{\Delta E} \tag{2.4}$$

where

$$\delta^e_{vert}(s) = \frac{2\alpha}{\pi}\left(\frac{3}{4}\ \ell n\ \frac{s}{m_e^2} - 1 + \frac{\pi^2}{6}\right) ,$$

$$\delta^\mu_{vert}(s) = \frac{2\alpha}{\pi}\left(\frac{3}{4}\ \ell n\ \frac{s}{m_\mu^2} - 1 + \frac{\pi^2}{6}\right) ,$$

$$t_e = \frac{2\alpha}{\pi}\left(\ell n\ \frac{s}{m_e^2} - 1\right) ,$$

$$t_\mu = \frac{2\alpha}{\pi}\left(\ell n\ \frac{s}{m_\mu^2} - 1\right) ,$$

$$t_{e\mu} = \frac{8\alpha}{\pi}\ \ell n\left(\tan\frac{\theta}{2}\right) .$$

θ is the angle between e^- and μ^-. $t_{e\mu}$ is asymmetric with respect to the plane perpendicular to the beam axis. δ_A is the asymmetric and noninfrared divergent part of the radiative corrections:

$$\delta_A(\theta) = \frac{2\alpha}{\pi}\left\{-\frac{2}{1+\cos^2\theta}\left[\cos\theta\left\{\ell n^2\left(\sin\frac{\theta}{2}\right) + \ell n^2\left(\cos\frac{\theta}{2}\right)\right\} + \sin^2\frac{\theta}{2}\ \ell n\left(\cos\frac{\theta}{2}\right)\right.\right.$$
$$\left.\left. - \cos^2\frac{\theta}{2}\ \ell n\left(\sin\frac{\theta}{2}\right)\right] + 2\ \ell n^2\left(\sin\frac{\theta}{2}\right) - 2\ \ell n^2\left(\cos\frac{\theta}{2}\right) - \Phi\left(\sin^2\frac{\theta}{2}\right) + \Phi\left(\cos^2\frac{\theta}{2}\right)\right\} ,$$

where $\Phi(x)$ is the Spence function (also called dilogarithm). The numerical values of $\delta_A(\theta)$ are shown in Table I. δ_A and $t_{e\mu}$ are both odd with respect to the interchange $\mu^+ \leftrightarrow \mu^-$ and hence contribute only to the asymmetry but not to the total cross section up to order α^3 in the cross section. δ^e_{vert} and δ^μ_{vert} represent respectively the electron and muon vertices, t_e and t_μ represent the equivalent radiator thickness for electron and muon bremsstrahlungs respectively.

Π is the lowest order vacuum polarization contribution. The bubble in the vacuum polarization diagram could be an electron pair, a muon pair, a τ pair, or hadronic

states. The contributions from these various states, denoted by X, can be calculated from the cross section $\sigma_{ee\to X}(s)$ in the following way:

$$2\Pi(s) = \sum_X \delta^X_{vac}(s) \quad , \tag{2.5}$$

$$\delta^X_{vac}(s) = \frac{s}{2\pi^2\alpha}\, Re \int_{s_{th}}^{\infty} \frac{\sigma_{ee\to X}(s')\, ds'}{s - s' - i\epsilon} \quad , \tag{2.6}$$

where s_{th} is the threshold value of s for the production of the final state X and Re stands for the real part. For a lepton pair with mass m we have $s_{th} = 4m^2$,

$$\sigma_{ee\to\ell\ell}(s) = \frac{4\pi\alpha^2}{3s}\,\beta\,\frac{3-\beta^2}{2} \quad , \quad \text{with } \beta^2 = 1 - \frac{4m^2}{s} \quad ,$$

and we thus obtain from Eq. (2.6),

$$\delta^\ell_{vac}(s) \equiv \frac{2\alpha}{\pi}\, f(x)$$

with $x = s_{th}/s$ and

$$f(x) = -\frac{5}{9} - \frac{x}{3} + \frac{(1-x)^{1/2}(2+x)}{6}\, \ell n \left|\frac{(1-x)^{1/2}+1}{(1-x)^{1/2}-1}\right| \quad \text{if } x \le 1 \quad , \tag{2.7}$$

and

$$f(x) = -\frac{5}{9} - \frac{x}{3} + \frac{(x-1)^{1/2}(2+x)}{3}\, \tan^{-1}\frac{1}{(x-1)^{1/2}} \quad \text{if } x > 1 \quad . \tag{2.8}$$

Since we are interested in energy range $s \gg 4m_\mu^2$, we have

$$\delta^e_{vac}(s) = \frac{2\alpha}{\pi}\left(\frac{1}{3}\,\ell n\,\frac{s}{m_e^2} - \frac{5}{9}\right) \quad , \tag{2.9}$$

$$\delta^\mu_{vac}(s) = \frac{2\alpha}{\pi}\left(\frac{1}{3}\,\ell n\,\frac{s}{m_\mu^2} - \frac{5}{9}\right) \quad , \tag{2.10}$$

$$\delta^\tau_{vac}(s) = \frac{2\alpha}{\pi}\, f(x_\tau) \quad \text{with } x_\tau = \frac{4m_\tau^2}{s} \quad . \tag{2.11}$$

Let us next consider the hadronic contributions to the vacuum polarization. For the nonresonant region, $\sigma_{e^+e^-\to had}(s)$ can be roughly represented by $1.2\,\sigma_{e^+e^-\to quark\ partons}$,

hence we may write δ_{vac}^{had} in terms of the function $f(x)$ given above in the following way:

$$\delta_{vac}^{had}(s) = 1.2\ \frac{2\alpha}{\pi}\left\{\frac{5}{3}\ f(x_u) + \frac{1}{3}\ f(x_s) + \frac{4}{3}\ f(x_c) + \frac{1}{3}\ f(x_b)\right\}\ , \qquad (2.12)$$

where x_u, x_s, x_c and x_b are s_{th}/s for production of different quark flavors and are given approximately by $x_u = 4m_\pi^2/s$, $x_s = 1\ GeV^2/s$, $x_c = 9\ GeV^2/s$ and $x_b = 100\ GeV^2/s$.

The contribution to δ_{vac} from hadronic resonances can be estimated by substituting the Breit-Wigner formula:

$$\sigma_{e^+e^-\to Res}(s) = \frac{\Gamma(R\to e^+e^-)\ \Gamma_t\ 12\pi}{(s-M_R^2)^2+\Gamma_t^2\ M_R^2}\ \underset{\Gamma_t\to 0}{\to}\ \frac{12\pi^2}{M_R}\ \Gamma(R\to e^+e^-)\ \delta(s-M_R^2) \qquad (2.13)$$

into Eq. (2.6). We obtain

$$\begin{aligned}\delta_{vac}^{Res}(s) &= \frac{6\Gamma(R\to e^+e^-)}{\alpha M_R}\ \frac{s[s-M_R^2+\Gamma_t M_R\pi^{-1}\ell n(s/M_R^2)]}{(s-M_R^2)^2+\Gamma_t^2 M_R^2} \\ &\underset{\Gamma_t\to 0}{\to} \frac{6\Gamma(R\to e^+e^-)}{\alpha M_R}\ \frac{s}{s-M_R^2}\ .\end{aligned} \qquad (2.14)$$

In Table II we list all the known resonances in $e^+e^- \to$ hadrons, together with their masses M_R, total widths Γ_t, the partial widths into e^+e^-, $\Gamma(R\to e^+e^-)$, and the quantities $6\Gamma(R\to e^+e^-)/(\alpha M_R)$ which appear in Eq. (2.14). We note that the contribution of these resonances to δ_{vac} is not important except in the neighborhood of the resonance. Its effect is to increase the high energy side and deplete the low energy side of the resonance peak. Since the bremsstrahlung effect increases the high energy side of the peak with much higher strength (factor of 100 to 1000) we will not see the effect of δ_{vac}^{Res} at high energy side of the peak. We should be able to see a slight dip in the cross section at the low energy side.

The asymmetric term $t_{e\mu}$ was first obtained by Tsai (Tsai, 1965). The expression for $\delta_A(\theta)$ was obtained by Khriplovich (Khriplovich, 1973), Discus (Discus, 1973) and Brown et al. (Brown, 1973). The hadronic contributions to the vacuum polarization were treated by Tsai (Tsai, 1960), Cabibbo and Gatto (Cabbibo, 1961), and Berends and Gastmans (Berends, 1978).

B. Radiative Corrections to All Orders to $e^+e^- \to \mu^+\mu^-$

In this subsection we apply our modified renormalization group formula Eq. (2.3) to the radiative corrections to $e^+e^- \to \mu^+\mu^-$. The purpose is to demonstrate the properties of (2.3).

1. Reproduction of the lowest order radiative corrections

To order α in radiative corrections Eq. (2.3) reproduces Eq. (2.1) exactly, including all the masses. If all the masses of charged lines are set equal to λ^2 in (2.3), it reproduces the results of (2.2). Thus (2.3) is the most natural extension of (2.1) and (2.2).

2. Factorization

Equation (2.3) can be decomposed into products of factors, each of which has a well defined physical meaning:

$$\begin{aligned}\left(\frac{1}{1-\Pi}\right)^{2+(A/\Pi)} &= (1-\Pi)^{-2} \\ &\times (1-\Pi)^{t_e \ell n(E/\Delta E)/\Pi}\,(1-\Pi)^{-\delta^e_{vert}/\Pi} \\ &\times (1-\Pi)^{t_\mu \ell n(E/\Delta E)/\Pi}\,(1-\Pi)^{-\delta^\mu_{vert}/\Pi} \\ &\times (1-\Pi)^{t_{e\mu} \ell n(E/\Delta E)/\Pi}\,(1-\Pi)^{-\delta_A/\Pi}\ .\end{aligned} \tag{2.15}$$

This is consistent with the fact that we could have applied the renormalization group technique to each of these factors instead of σ/σ_0. In Eq. (2.15) we have arranged the factors into four lines to indicate that in principle factors in each line should be considered together because of infrared cancellations. By infrared cancellations we meen cancellation of all infrared factors $K(p_i, p_j)$ defined by Eq. (A.30). The physical meaning of each factor is discussed subsequently.

3. Multiphoton Exchange

The two photon exchange diagrams and the interference terms between initial and final state bremsstrahlung diagrams are given by δ_A and $t_{e\mu}$ and they do not have mass singularities. Therefore it is natural to expect that all the mass singularities in multiple photon exchange and the interference terms between initial and final state multiphoton bremsstrahlung do not have leading log mass singularities. Equation (2.3) has this property as can be seen by expanding the last two factors in Eq. (2.15).

4. Vacuum polarization in the main photon propagator

The factor $(1-\Pi)^{-2}$ in Eq. (2.15) is the square of the chain sum of the vacuum polarization diagrams in the main photon propagator in the reaction $e^+e^- \to \mu^+\mu^-$.

5. Elastic vertex function

The factor with the electron vertex δ^e_{vert} in (2.15) can be written as

$$\begin{aligned}(1-\Pi)^{-\delta^e_{vert}/\Pi} &= exp\ [\delta^e_{vert}\ \Pi^{-1}\ \ell n(1-\Pi)^{-1}] \\ &= 1+\delta^e_{vert}[-\Pi^{-1}\ \ell n(1-\Pi)] \\ &\quad + \frac{(\delta^e_{vert})^2}{2!}\ [-\Pi^{-1}\ \ell n(1-\Pi)]^2 \\ &\quad + \frac{(\delta^e_{vert})^3}{3!}\ [-\Pi^{-1}\ \ell n(1-\Pi)]^3 \\ &\quad + \frac{(\delta^e_{vert})^4}{4!}\ [-\Pi^{-1}\ \ell n(1-\Pi)]^4 + \ldots \quad .\end{aligned} \tag{2.16}$$

Each term in the above expansion can again be expanded in the following way:

$$\delta^e_{vert}[-\Pi^{-1}\ \ell n(1-\Pi)] = \delta^e_{vert}\left(1+\frac{1}{2}\ \Pi+\frac{1}{3}\ \Pi^2+\ldots\right) \quad , \tag{2.17}$$

which can be identified with the interference terms between the lowest order diagram M_0 and the sum of vertex diagrams, $M_v + M_{v1} + M_{v2} + M_{v3} + \ldots$ as shown in Fig. 1. In order to save us from drawing too many pictures, we use one Feynman diagram to represent the sum of all gauge invariant subset of diagrams. The third term in the expansion of (2.16) can be identified with two classes of diagrams shown in Fig. 2(a) where a square box represents the sum of chain diagrams of vacuum polarizations as shown in Fig. 1. The fourth and the fifth terms in (2.16) are shown in Figs. 2(b) and 2(c) respectively.

The identification of terms appearing in Eqs. (2.16) and (2.17) with various Feynman diagrams have not been proven rigorously. Let us indicate how this can be qualitatively understood by investigating the simplest diagram M_{v1} of Fig. 1 and see whether it is given by the term $(1/2)\delta^e_{vert}\Pi$ of (2.17).

The electron vertex function M_v of Fig. 1 contains integrations of the form

$$J_{(1,2,3)} = \int (1;\ \ell_\sigma;\ \ell_\sigma\ell_\tau)\ \ell^{-2}\ d^4\ell\ [(P_1-\ell)^2-m_e^2]^{-1}\ [(P_2+\ell)^2-m_e^2]^{-1} \quad . \tag{2.18}$$

The corresponding expression of the integrations for M_{v1} in Fig. 1 is obtained by inserting the vacuum polarization function $\Pi(\ell^2)$ in the integrand. Thus all we need to prove is that the integrand in (2.18) multiplied by $\Pi(\ell^2)$ is dominated by the region $\ell = \pm(P_1+P_2) = \pm q$ and that the dominance is not very peaked so that we have to put a factor 1/2 in front. The integration with 1 as the numerator is infrared divergent and is cancelled completely by exactly the same function occuring in the electron bremsstrahlung $|M_b|^2$ of Fig. 3 and thus does not contribute to δ^e_{vert}. When $\Pi(\ell^2)$ is inserted into the integrand, it eliminates the infrared divergence because as $\ell^2 \to 0$, $\Pi(\ell^2) \sim \ell^2$. The integration with ℓ_σ as the numerator is finite both in the infrared and ultraviolet regions and the integration is indeed dominated by the regions near $\ell = \pm(P_1 + P_2)$. The integration with $\ell_\sigma \ell_\tau$ in the numerator is ultraviolet divergent which is usually cut off by the renormalization procedure. After the renormalization the integration is indeed dominated by the regions near $\ell = \pm(P_1 + P_2)$. The factor 1/2 can be understood in the following way. We notice that $\Pi(\ell^2)$ is a logarithmic function of ℓ^2. Now δ^e_{vert} is also a logarithmic function of q^2 as a result of integration with respect to ℓ^2, and thus the integral must behave approximately $d\ell^2/\ell^2$. Thus the factor of 1/2 can be understood easily from the fact that (this was pointed out by M. Peskin to the author)

$$\int_1^x \frac{dx}{x}\, \ell n\, x = \frac{1}{2}\, \ell n^2 x \quad .$$

The higher order terms in (2.17) can then be understood from the relation

$$\int_1^x \frac{dx}{x}\, \ell n^n x = \frac{1}{n+1}\, \ell n^{n+1} x \quad . \tag{2.19}$$

If we ignore the vacuum polarization in (2.16) and (2.17), then (2.16) reduces to $exp\ (\delta^e_{vert})$. This solves one of the long standing question in radiative corrections, namely, what part of the lowest order radiative correction should one exponentiate? Equation (2.3) tells us that we should exponentiate not only the bremsstrahlung, as originally conjectured by Schwinger (Schwinger, 1949) and later proven by Yennie, Frautschi and Suura (Yennie, 1961), but also the vertex part. It also tells us that the vacuum polarization part should not be exponentiated, rather it should be summed chainwise and written in the form $(1-\Pi)^{-2}$ as given by Eq. (2.3).

6. Bremsstrahlung and pair conversions

The factor in Eq. (2.15) with the equivalent radiator thickness t_e represents the bremsstrahlung and the pair conversions as shown in Figs. 3 and 4. In order to establish a one to one correspondence of different expansion terms of this factor with Feynman diagrams, we again write it in an exponential form and then expand it in power series:

$$\begin{aligned}(1-\Pi)^{t_e \ell n(E/\Delta E)/\Pi} &= exp\,[-t_e\,\ell n(E/\Delta E)\,\Pi^{-1}\,\ell n(1-\Pi)^{-1}] \\ &= 1+[-T\,\ell n(E/\Delta E)]+[-T\,\ell n(E/\Delta E)]^2/2! \\ &\quad +[-T\,\ell n(E/\Delta E)]^3/3!+\ldots\ ,\end{aligned} \tag{2.20}$$

where T is a new equivalent radiator which contains not only the effect due to the bremsstrahlung but also the effect due to its conversion into a pair of $e^{\pm}$, $\mu^{\pm}$, $\tau^{\pm}$, $d^{\pm}$, $u^{\pm}$, etc.

$$\begin{aligned}T &= t_e\,\Pi^{-1}\,\ell n(1-\Pi)^{-1} \\ &= t_e\Big(1+\frac{1}{2}\,\Pi+\frac{1}{3}\,\Pi^2+\ldots\Big)\ .\end{aligned} \tag{2.21}$$

The values of t_e, Π and T in % are tabulated in Table III. We notice that the increase in equivalent radiator thickness due to pair conversions is very small, the difference between T and t_e is of order 0.2 to 0.4% for $\sqrt{s}=20$ to 200 GeV.

We notice that the term $-T\,\ell n(E/\Delta E)$ contributes negatively to the cross section. In the bremsstrahlung case we know that the vertex diagram has a large negative infrared term which cancels out with the infrared term in the bremsstrahlung. After this cancellation we assign a positive number δ^e_{vert} to the vertex correction and a negative number $-t_e\ell n(E/\Delta E)$ to the bremsstrahlung correction. Similarly the negative number coming from the rest of the expansion:

$$-T\,\ell n(E/\Delta E)-[-t_e\,\ell n(E/\Delta E)]=-t_e\,\ell n(E/\Delta E)\left(\frac{1}{2}\,\Pi+\frac{1}{3}\,\Pi^2+\frac{1}{4}\,\Pi^3+\ldots\right)$$

represents the internal conversion of "a" virtual photon into a pair (see Fig. 3, $|M_{b1}+M_{b2}+\overline{M}_{b3}+\ldots|^2$) after cancellation with diagrams shown in Fig. 1 $M_{v1}, M_{v2},\ldots$. Since it is a nontrivial matter to do all these calculations, we differentiate $-T\,\ell n(E/\Delta E)$

with respect to ΔE, the result is now positive and should represent the contributions from inelastic diagrams shown in Fig. 3:

$$\frac{d}{d(\Delta E)}\,[-T\,\ell n(E/\Delta E)] = (t_e/\Delta E)\left(1+\frac{1}{2}\,\Pi+\frac{1}{3}\,\Pi^2+\frac{1}{4}\,\Pi^3+\ldots\right)$$

where $t_e/\Delta E$ comes from the bremsstrahlung diagram $|M_b|^2$ of Fig. 3 and $(t_e/\Delta E)$ $[(1/2)\Pi + (1/3)\Pi^2 + (1/4)\Pi^3 + \ldots]$ should represent the pair conversion diagrams $|M_{b1} + M_{b2} + M_{b3} + \ldots|^2$ of Fig. 3.

When pair conversion is ignored, T is replaced by t_e and Eq. (2.20) gives the well known exponential form of the infrared photon cross section. I regard this as one of the triumph of the renormalization group technique. With the inclusion of the pair conversion, ΔE now represents the energy loss due to emission of photons and pairs.

Let q' be the four momentum of the virtual photon coupled to the pair. If we assume that the matrix elements of emitting the virtual photon q' is independent of q'^2 (often called the pole dominance model) we may use the Kroll-Wada relation (Kroll, 1955) to write the internal pair conversion probability as (see Fig. 3 for notations)

$$|M_{b1}|^2 = |M_b|^2\,\frac{\alpha}{3\pi}\int_{q'^2_{min}}^{q'^2_{max}}\frac{dq'^2}{q'^2} \approx |M_b|^2\,\Pi[(\Delta E)^2] \tag{2.22}$$

where $q'^2_{max} = (\Delta E)^2$ and $q'^2_{min} = 4m^2$. (For simplicity we have assumed that only one kind of fermion pair with mass m and charge e participate in both the vacuum polarization and the pair conversion. The argument can be generalized to the actual case where many different particles participate in both the vacuum polarization and the pair conversion.)

Inserting the chain-sum of the vacuum polarization diagrams into the photon propagator in (2.22), we obtain

$$\begin{aligned}|M_{b1} + M_{b2} + M_{b3} + \ldots|^2 &= |M_b|^2\,\frac{\alpha}{3\pi}\int_{4m^2}^{(\Delta E)^2}\left[1-\frac{\alpha}{3\pi}\,\ell n\!\left(\frac{q'^2}{m^2}\right)\right]^{-2}\frac{dq'^2}{q'^2}\\ &= |M_b|^2\left[\Pi((\Delta E)^2)+\Pi^2((\Delta E)^2)+\Pi^3((\Delta E)^2)+\ldots\right]\end{aligned} \tag{2.23}$$

which is to be compared with (2.21), which gives:

$$|M_b|^2\left(\frac{1}{2}\,\Pi(s)+\frac{1}{3}\,\Pi^2(s)+\frac{1}{4}\,\Pi^3(s)+\ldots\right)\quad . \tag{2.24}$$

Equations (2.23) and (2.24) are not the same, but they are related. If we integrate both expressions with respect to ΔE from the threshold 2m to its maximum possible value $\sqrt{s}$, remembering that $|M_b|^2$ is proportional to $(\Delta E)^{-1}$, we obtain the same answers. When $(\Delta E)^2 < 2Em$ (2.24) is larger than (2.23), but when $(\Delta E)^2 > 2Em$ the reverse is true. In general the matrix element of emitting a virtual photon q' is not independent of q'^2 as was assumed in obtaining the Kroll-Wada relation (2.22). It is suppressed when q'^2 is large so this will partially correct the above result in the right direction. In order to do a more complete justification of (2.20) and (2.21) we need to do a complete calculation and I have not done it. However the result as it stands is already very impressive. We notice that pair conversion does not occur in the lowest order radiative corrections which were the starting point of our calculation. Therefore we conclude that the renormalization group technique predicts the existence of pair conversion and very likely predicts its magnitude correctly.

The terms with higher power of t_e in (2.20) of course represent the multiple photon emission and their conversions into pairs. Some of the diagrams associated with t_e^2 are shown in Fig. 4.

7. Kinoshita-Lee-Nauenberg cancellations

Kinoshita (Kinoshita, 1962) and Lee and Nauenberg (Lee, 1964) observed that if one sums over all the states with the same energy (degenerate states) the mass singularities cancel out to all orders in perturbation theory, provided we ignore the mass singularities coming from the vacuum polarizations. In our problem the initial state is preselected by the machine so that e^+ and e^- have a definite energy E each. Thus the mass singularity due to initial state radiative corrections remains. The final states can be summed and after doing so we expect their mass singularity to cancel to all orders in perturbation theory. This actually happens in our formalism. To see this we need the photon spectrum valid for a hard photon emission. This can be written as (see for example Bjorken, 1963)

$$t_\mu \frac{1}{2} [1 + (1-x)^2] x^{-1} dx \quad , \tag{2.25}$$

where $x = k/E$ and t_μ is defined in (2.4). Integrating (2.25) with respect to x from $\Delta E/E$ to 1, we obtain

$$\int_{\Delta E/E}^{1} t_\mu \left(x^{-1} - 1 + \frac{1}{2} x \right) dx \approx t_\mu \left(\ell n \frac{E}{\Delta E} - \frac{3}{4} \right) \quad . \tag{2.26}$$

Adding (2.26) to the final state part of the lowest order radiative corrections given by (2.4) and calling it A_f we obtain

$$A_f = \delta^{\mu}_{vert} - t_\mu \, \ell n \, \frac{E}{\Delta E} + t_\mu \left(\ell n \, \frac{E}{\Delta E} - \frac{3}{4} \right) = \frac{2\alpha}{\pi} \left(-\frac{1}{4} + \frac{\pi^2}{6} \right) \quad , \tag{2.27}$$

which no longer has any mass singularity. Applying the renormalization group technique, this result can then be extended to all orders:

$$(1-\Pi)^{-A_f/\Pi} = exp\,[A_f\,\Pi^{-1}\,\ell n(1-\Pi)^{-1}] = exp\left[A_f\left(1+\frac{1}{2}\,\Pi+\frac{1}{3}\,\Pi^2+\ldots\right)\right] \quad . \tag{2.28}$$

The mass singularity in Π, which can be either due to the vacuum polarization or pair conversion in (2.28) does not contribute to the leading log because A_f is of order α and does not have logarithmic terms. We conclude that the radiative corrections to the final states are negligible if we sum over the final states.

This is very significant when dealing with hadronic final states which are usually too complicated to be radiatively corrected. Our results indicate that we can ignore the radiative corrections to the final hadronic states completely. We need to consider only the vacuum polarization correction to the main photon propagator and the initial state radiative corrections.

In our problem the mass singularities from initial state bremsstrahlung t_e and the initial state vertex δ^{e}_{vert} do not cancel each other out when the photon spectrum is integrated because as the bremsstrahlung is emitted from the initial electron the virtual photon four momentum is changed from s to $s' = s(1-k/E)$. Since the cross section for $e^+e^- \to \mu^+\mu^-$ is inversely proportional to s', we have to multiply a factor $(1-x)^{-1}$ to the integrand of Eq. (2.26). Thus the mass singularity of the resulting expression does not cancel with that from δ^{e}_{vert}. In the language of Lee and Nauenberg we do not expect any cancellation for the initial state because we are not summing over all the degenerate initial states, the machine preselects the electron and the positron to have energy E each, and no other degenerate state participates in the interaction. These two ways of explaining the failure of cancellation of mass singularities in the initial state radiative corrections are independent of each other, namely one is not a consequence of the other.

I regard it also as one of the triumphs of the renormalization group technique to be able to exhibit the Kinoshita-Lee-Nauenberg cancellation in the QED problem.

8. Higher order corrections to the asymmetry

Let us consider the radiative corrections to the θ asymmetry. As θ is changed into $(\pi-\theta)$, the asymmetric part $A_a = \delta_A - t_{e\mu}\,\ell n(E/\Delta E)$ in A of (2.4) changes sign. Thus in the asymmetry all other factors in Eq. (2.15) cancel out and we obtain

$$\frac{\sigma(\theta)-\sigma(\pi-\theta)}{\sigma(\theta)+\sigma(\pi-\theta)} = \frac{(1-\Pi)^{-A_a/\Pi}-(1-\Pi)^{+A_a/\Pi}}{(1-\Pi)^{-A_a/\Pi}+(1-\Pi)^{+A_a/\Pi}} \tag{2.29}$$

$$\approx [\delta_A - t_{e\mu}\,\ell n(E/\Delta E)]\left(1+\frac{1}{2}\,\Pi\right) \tag{2.30}$$

where δ_A, $t_{e\mu}$ and Π are defined in (2.4) and the values of δ_A and Π are tabulated in Tables I and III respectively. The physical origins of the correction are twofold. The term $\frac{1}{2}\Pi\delta_A$ comes from the fact that in the two photon exchange both photons can have vacuum polarization and the term $-\frac{1}{2}\Pi t_{e\mu}\ell n(E/\Delta E)$ comes from the interference between the internal pair conversions from the initial electron and the final muon lines represented by Feynman diagrams $M_{d1}^{\dagger}\,M_{d2}+M_{d2}^{\dagger}\,M_{d1}$ shown in Fig. 5(d). As shown in Table III, Π is about 5% at $\sqrt{s}=30$ GeV, hence the correction to the asymmetry is only about 2.5%. It is nice to know that the correction is small.

III. RADIATIVE CORRECTIONS TO HARD PHOTON PROCESSES

When the energy loss due to radiation is large the cross section can no longer be written as a simple product of the lowest order Born cross section times a factor as shown in (2.1) and (2.2). The lowest order cross section for $e^+e^- \to \mu^+\mu^-\gamma$ can be obtained using Feynman diagrams $M_{b1} + M_{b2}$ shown in Fig. 5(b). An approximate formula was given by Berends, Gastmans and Wu (Berends, 1969) for the matrix elements squared which is shown below:

$$d\sigma = \frac{4\alpha^3}{s\pi^2}\int \frac{d^3P_3}{2E_3}\int \frac{d^3P_4}{2E_4}\int \frac{d^4k}{2k}\,\delta^4(P_1+P_2-P_3-P_4-k)\,|M_{b1}+M_{b2}|^2 \qquad (3.1)$$

with

$$M_{b1}^{\dagger}\,M_{b1} = -\frac{m_\mu^2}{2s^2}\left[\frac{t^2+u'^2}{(P_3\cdot k)^2}+\frac{t'^2+u^2}{(P_4\cdot k)}\right]+\frac{t^2+t'^2+u^2+u'^2}{4s(P_3\cdot k)(P_4\cdot k)} \qquad (3.2)$$

$$M_{b2}^{\dagger}\,M_{b2} = -\frac{m_e^2}{2s'^2}\left[\frac{t^2+u^2}{(P_1\cdot k)^2}+\frac{t'^2+u'^2}{(P_2\cdot k)^2}\right]+\frac{t^2+t'^2+u^2+u'^2}{4s'(P_1\cdot k)(P_2\cdot k)} \qquad (3.3)$$

$$2M_{b1}^{\dagger}\,M_{b2} = \frac{t^2+t'^2+u^2+u'^2}{4ss'} \qquad (3.4)$$

$$\times\left[-\frac{t}{(P_2\cdot k)(P_4\cdot k)}-\frac{t'}{(P_1\cdot k)(P_3\cdot k)}+\frac{u'}{(P_1\cdot k)(P_4\cdot k)}+\frac{u}{(P_2\cdot k)(P_3\cdot k)}\right]$$

and

$$t = (P_2-P_4)^2 \quad , \quad t' = (P_1-P_3)^2 \quad , \quad u = (P_2-P_3)^2$$

$$u' = (P_1-P_4)^2 \quad , \quad s = (P_1+P_2)^2 \quad , \quad s' = (P_3+P_4)^2 \quad .$$

P_1, P_2, P_3 and P_4 refer to four momenta of e^-, e^+, μ^- and μ^+ respectively. We have also calculated the exact expression for $|M_{b1}+M_{b2}|^2$ using Hearn's reduce program. The exact expression is about 100 times more complicated than expressions shown in (3.2), (3.3) and (3.4) but numerically the latter yields results accurate to within one part in 3000 compared with the exact α^3 calculation in the kinematical range we have checked. $2M_{b1}^{\dagger}\,M_{b2}$ given in (3.4) is odd under the exchange $\mu^+ \leftrightarrow \mu^-$ and thus it contributes only to the asymmetry and not to the total cross section. The Monte Carlo program using Eqs. (3.1) to (3.4) was written by Berends and Kleiss (Berends, 1981)

which is very convenient for experimentalists because it can handle any experimental cuts in energy and angle. Thus we would like to write a prescription for doing higher order effects which can be adopted easily to the Monte Carlo program of Berends and Kleiss.

In order to do this, let us differentiate (2.3) with respect to ΔE. We obtain [see (2.21)]

$$\left[\frac{\partial\sigma}{\partial(\Delta E)}\right]_{\Delta E=k} = \frac{(t_e+t_\mu+t_{e\mu})}{k}\,\sigma_0\left(\frac{1}{1-\Pi}\right)^{2+(A/\Pi)}\left(1+\frac{1}{2}\,\Pi+\frac{1}{3}\,\Pi^2+\ldots\right) \quad . \tag{3.5}$$

The lowest order cross section (order α^3) in the above formula is $(t_e+t_\mu+t_{e\mu})\sigma_0/k$, hence the factor

$$\left(\frac{1}{1-\Pi}\right)^{2+(A/\Pi)}\left(1+\frac{1}{2}\,\Pi+\frac{1}{3}\,\Pi^2+\ldots\right) \tag{3.6}$$

can be regarded as the radiative corrections to Eq. (3.1) in the soft photon limit. The physical meaning of the factor $[1/(1-\Pi)]^{2+(A/\Pi)}$ is similar to the one given in Sec. II except now we are dealing with the radiative corrections to the bremsstrahlung diagram $M_{b1}+M_{b2}$ in stead of the elastic diagram M_0 shown in Fig. 5(a). The physical meaning of the factor $(1+(1/2)\Pi+(1/3)\Pi^2+\ldots)$ was already discussed in the previous chapter [Eqs. (2.21) to (2.24)], namely the term 1 gives the bremsstrahlung, and the term $(1/2)\Pi+(1/3)\Pi^2+\ldots$ gives the pair conversion of the bremsstrahlung represented by $|M_{b1}+M_{b2}+M_{b3}+\ldots|^2$ in Fig. 3.

Since the final states observed could be $\mu^+\mu^-\gamma$, $\mu^+\mu^-e^+e^-$, $\mu^+\mu^-\mu^+\mu^-$, $\mu^+\mu^-$ hadrons etc., let us sketch how (3.5) and (3.1) can be combined to describe different experimental situations.

<u>$e^+e^- \to \mu^+\mu^-\gamma$</u>

Since a high energy γ is observed, we know it is not converted into a pair. In this case we should retain only the term 1 and discard $(1/2)\Pi+(1/3)\Pi^2+\ldots$ in (3.6). Let us assume that the cut used is that the total energy of μ^+, μ^- and γ added is within ΔE of the total energy $2E$

$$2E-(E_3+E_4+k) \;<\; \Delta E \ll E \quad .$$

The correction factor $(1-\Pi)^{-2-A/\Pi}$ is a function of the virtual photon energy in the main photon propagator and the latter can be either s or $s' = s(1-k/E)$ depending

upon whether the photon is emitted by the final muon system or initial electron system. Defining

$$F(s) = [1 - \Pi(s)]^{-2-A(s)/\Pi(s)}$$

then the radiative corrections to the α^3 cross section (3.1) under the present experimental condition is obtained by multiplying $F(s)$, $F(s')$ and $[F(s)\ F(s')]^{1/2}$ to $M_{b1}^{\dagger} M_{b1}$, $M_{b2}^{\dagger} M_{b2}$ and $2M_{b1}^{\dagger} M_{b2}$ respectively.

We notice that this procedure gives the correct Bloch-Nordsieck limit, namely as $\Delta E \to 0$ the cross section becomes zero. Physically this is due to the fact that the cross section for emitting any finite number of photons (in this case 1) is zero, because in any physical process involving charged particles, there are always infinitely many photons emitted.

$\underline{e^+e^- \to \mu^+\mu^-\mu^+\mu^-}$

In this case the photon is definitely converted into a muon pair so the factor $[1 + (1/2)\Pi + (1/3)\Pi^2 + \ldots]$ in (3.5) and (3.6) should be replaced by

$$\Pi_\mu \left(\frac{1}{2} + \frac{1}{3}\,\Pi + \frac{1}{4}\,\Pi^2 + \ldots\right) \equiv f_\mu(s) \quad ,$$

where Π_μ is equal to the muon part of Π given by

$$\Pi_\mu = \frac{\alpha}{3\pi}\left(\ell n\ \frac{s}{m_\mu^2} - \frac{5}{3}\right) \quad .$$

Suppose the experimental cut is such that

$$2E - (\text{sum of the muon energies}) < \Delta E \quad .$$

Then according to our prescription the cross section for $e^+e^- \to \mu^+\mu^-\mu^+\mu^-$ can be obtained by multiplying $f_\mu(s)F(s)$, $f_\mu(s')F(s')$ and $[f_\mu(s)\ F(s)\ f_\mu(s')\ F(s')]^{1/2}$ onto $M_b^{\dagger} M_{b1}$, $M_{b2}^{\dagger} M_{b2}$, and $2M_{b1}^{\dagger} M_{b2}$ of Eq. (3.1) respectively.

IV. RADIATIVE CORRECTIONS TO $e^+e^- \rightarrow$ HADRON CONTINUUM

For this type of reactions we perform only the radiative corrections to the initial e^+e^- system and the vacuum polarization corrections to the main photon propagator which is coupled to the final hadrons. The reasons for not doing radiative corrections to the final hadronic system are twofold. In the first place the hadronic final system is very complicated and since the radiative corrections depend upon the detail of how the experiment is done, it is difficult to give a general prescription for them. The second reason is that our understanding of the hadronic problem is so crude that there is no need to worry about the electromagnetic corrections. In any case if we find later that it is necessary to do radiative corrections to the hadronic states for some specific problem we can do the calculation then, because the initial state radiative corrections and the final state radiative corrections can be decoupled to a large extent. For measurement of $R = \sigma(e^+e^- \rightarrow \text{hadrons})/\sigma(e^+e^- \rightarrow \mu^-\mu^+)$ we do not need to perform the final state radiative corrections because of the Kinoshita-Lee-Nauenberg cancellations as explained previously in Sec. II.B.7.

Let $W = 2E$ be the sum of energies of e^+ and e^- beams and $s = W^2$. Since part of the energy is lost through the emission of photons and the internal conversions of photons into pairs, the center-of-mass energy of e^+e^- before annihilation becomes W' which is less than W. Let $\sigma_0(W')$ be the lowest order cross section for $e^+e^- \rightarrow$ hadron at energy W'. The experimental cross section is then

$$\sigma_{exp}(W) = \int_0^{x_{max}} \left[Tx^{T-1} \left(1 - x + \frac{x^2}{2}\right) \times \left[1 - \Pi(W'^2)\right]^{-2-\delta^e_{vert}(W'^2)/\Pi(W'^2)} \sigma_0(W') \right] dx \tag{4.1}$$

where

$$x = (W - W')/[(1/2)W] \quad , \tag{4.2}$$

$$T = \frac{2\alpha}{\pi}\left(\ell n \frac{W^2}{m_e^2} - 1\right) \frac{\ell n[1 - \Pi(W^2)]^{-1}}{\Pi(W^2)} \quad , \tag{4.3}$$

$$\delta^e_{vert}(W'^2) = \frac{2\alpha}{\pi}\left(\frac{3}{4}\, \ell n\, \frac{W'^2}{m_e^2} - 1 + \frac{\pi^2}{6}\right) \quad ,$$

and $\Pi(W'^2)$ is defined in (2.5) and its numerical values tabulated in Table III. x_{max} is determined by the energy cut W'_{min} used in selecting the final state

$$x_{max} = (W - W'_{min})/[(1/2)W] \quad .$$

The bremsstrahlung spectrum used in (4.1) is $Tx^{T-1}[1 - x + (1/2)x^2]\ dx$ which is valid for soft as well as hard photon emission. The equivalent radiator thickness T contains both the effects of bremsstrahlung as well as the internal pair conversion of the bremsstrahlung. The effect of pair conversion is very small. It increases the radiator thickness from t_e to T, the values of both quantities are tabulated in Table III.

V. RADIATIVE CORRECTIONS TO $e^+e^- \rightarrow$ VERY NARROW RESONANCE

In this and the next sections we deal with radiative corrections to formation of a resonance and its subsequent decay $e^+e^- \rightarrow R \rightarrow f$ where R could be ρ, ψ, Υ, etc. and f could be e^+e^-, $\mu^+\mu^-$, one particular mode or sum of all modes of hadronic decays etc. In this case the most important additional consideration is the energy spread of the colliding beam machine. This problem was considered by the author (Tsai, 1974) in conjunction with the analysis of the ψ. Similar work was done by Yennie (Yennie, 1975), and Jackson and Scharre (Jackson, 1975) almost simultaneously. In this paper we shall bring the subject up to date by making the treatment correct to all order in α in the leading log approximation. Since my original work is not easily available to people outside SLAC I shall repeat most of the contents of that work here.

Let the mean energy of the sum of e^+ and e^- beams be $W = 2E$ and let us denote the machine enegy distribution by $G(W, W')\ dW'$. $G(W, W')$ has a Gaussian form:

$$G(W, W') = \frac{1}{\sqrt{2\pi}\,\Delta}\ exp\left[-\frac{(W - W')^2}{2\Delta^2}\right] \quad , \tag{5.1}$$

where Δ is related to the full width at half maximum (FWHM) by

$$\Delta = (\text{FWHM})/2.3548 \quad . \tag{5.2}$$

Usually the Gaussian distribution of each beam is given:

$$G(E, E') = \frac{1}{\sqrt{2\pi}\ \sigma}\ exp\left[-\frac{(E - E')^2}{2\sigma^2}\right] \quad , \tag{5.3}$$

where σ is related to Δ by $\Delta = \sqrt{2}\ \sigma$. Numerically σ/E is 0.04% for SPEAR, 0.1% for PEP, 0.06% for CESR at Cornell and expected to be 0.2 to 0.5% for SLC at SLAC. (These numbers have been kindly supplied to the author by Dr. Karl Brown of SLAC.)

Let us denote by $B(W', W'')\ dW''$ the probability distribution of the c.m. energy after the bremsstrahlung emission (including internal pair conversion), W' being the energy before the bremsstrahlung. The energy loss by bremsstrahlung is $W' - W''$. Since energy loss is always positive we have

$$B(W', W'') = 0 \quad \text{if } W' - W'' < 0 \quad . \tag{5.4}$$

The expression for $B(W', W'')$ is given by differentiating (2.20) with respect to ΔE:

$$B(W', W'') = \left[T\ \frac{(2/W')^T}{(W' - W'')^{1-T}}\right] \theta(W' - W'') \tag{5.5}$$

where

$$T = \frac{2\alpha}{\pi}\left[\ell n\left(\frac{s}{m_e^2}\right) - 1\right] \Pi^{-1}\ \ell n\ (1 - \Pi)^{-1} \quad . \tag{5.6}$$

Let us express the cross section for the reaction $e^+e^- \to R \to f$ by a Breit-Wigner formula

$$\sigma_b(W) = \frac{\Gamma(R \to e^+e^-)\ \Gamma(R \to f)}{(W^2 - M_R^2)^2 + \Gamma_t^2\ M_R^2}\ 12\pi \tag{5.7}$$

where M_R is the mass of the resonance, $\Gamma(R \to e^+e^-)$, $\Gamma(R \to f)$, and Γ_t are partial widths of $R \to e^+e^-$, $R \to f$, and the total width respectively.

We introduce two kinds of definitions for the leptonic width. Let us consider the partial decay width of $R \to e^+e^-$. Of course strictly speaking there is no such a decay mode because e^+ and e^- are always accompanied by an infinite number of photons (Bloch, 1937). Now according to the discussions given in Sec. II.B.7, if we sum the vertex corrections and the bremsstrahlung all the leading logs from these two sources cancel out to all order in α. Thus we do not have to worry about the final state radiative corrections. Since the decay of this channel, unlike hadronic decay modes, has to go through a virtual photon we must include the vacuum polarization effect. For theoretical analysis, such as obtaining the strength of coupling between a photon

and the resonance, it is more convenient to deal with the lowest order in α width Γ_0 rather than the true experimental width Γ_{exp}. Two are related by

$$\Gamma_0(R \to e^+e^-) = \Gamma_{exp}(R \to e^+e^-)\,[1 - \Pi(M_R^2)]^2 \quad .$$

For hadronic decay modes, there is no vacuum polarization, so $\Gamma_0(R \to \text{hadrons}) = \Gamma_{exp}(R \to \text{hadrons})$. For our analysis it is more convenient to deal with Γ_{exp}, so we shall let all Γ's in (5.7) represent Γ_{exp}. $[1 - \Pi(s)]^2$ is 0.958 at the $\psi(3.1)$ but it is 0.89 at $\sqrt{s} = 50$ GeV according to the values of $\Pi(s)$ tabulated in Table III. Therefore we should be clear whether we are dealing with Γ_0 or Γ_{exp}. Since $\Gamma(R \to e^+e^-)$ already contains the vacuum polarization in our definition we should not correct it for vacuum polarization. Let us multiply $\sigma_b(W)$ by the vertex correction and call it σ_{eff}:

$$\sigma_{eff}(W) = \sigma_b(W)\left[1 - \Pi(W^2)\right]^{-\delta^e_{vert}(W^2)/\Pi(W^2)} \quad . \tag{5.8}$$

The desired relation between the experimentally observed cross section $\sigma_{exp}(W)$ and the cross section $\sigma_{eff}(W'')$ is given by

$$\begin{aligned}\sigma_{exp}(W) &= \int_0^\infty dW'' \int_{W''}^\infty dW'\, G(W,W')\, B(W',W'')\, \sigma_{eff}(W'') \\ &\equiv \int_0^\infty dW''\, F(W,W'')\, \sigma_{eff}(W'') \quad .\end{aligned} \tag{5.9}$$

The lower limit of the dW' integration comes from (5.4). $B(W',W'')$ is too singular at $W' = W''$ for computer evaluation of (5.9). This singularity can be eliminated with an integration by parts in the following way:

$$\begin{aligned}F(W,W'') &\equiv \int_{W''}^\infty dW'\, G(W,W')\, B(W',W'') \\ &= \frac{1}{\sqrt{2\pi}\,\Delta}\left(\frac{2\sqrt{2}\,\Delta}{W}\right)^T \int_0^\infty exp\,[-(y-z)^2]\, dz^T \\ &= \frac{2}{\sqrt{2\pi}\,\Delta}\left(\frac{2\sqrt{2}\;\Delta}{W}\right)^T \int_{-y}^\infty (x+y)^T\, xe^{-x^2}\, dx\end{aligned} \tag{5.10}$$

where $\overline{y} = (W - W'')/\sqrt{2}\,\Delta$. There is no singularity in the integrand of (5.10), hence it can be handled easily by a computer.

1. Narrow Resonance

When the total width of the peak Γ_t is much narrower than the machine width, such as for ψ, we may replace (5.7) by a δ function and obtain

$$\sigma_b(W) \underset{\Gamma_t \to 0}{\to} 12\pi^2 \frac{\Gamma(R \to e^+e^-)\,\Gamma(R \to f)}{(\Gamma_t\, M_R)} \delta(W^2 - M_R^2) \quad . \tag{5.11}$$

Substituting (5.11) into (5.8) and (5.9) we obtain

$$\sigma_{exp}(W) = F(W, M_R)\, 6\pi^2 \frac{\Gamma(R \to e^+e^-)\,\Gamma(R \to f)}{(\Gamma_t\, M_R^2)} \left[1 - \Pi(M_R^2)\right]^{-\delta^e_{vert}(M_R^2)/\Pi(M_R^2)} . \tag{5.12}$$

In general the experimental resonance cross section will look like Fig. 6, where W is the energy of the machine at the Gaussian peak. The nonresonant background must be subtracted before applying (5.12). Except for the normalization the shape of $\sigma_{exp}(W)$ is determined completely by $F(W, M_R)$. The peak of the curve is given by $F(W, M_R)$ at $W = M_R$:

$$F(M_R, M_R) = \frac{1}{\sqrt{2\pi}\,\Delta} \exp\left(-T\, \ell n\, \frac{W}{2\sqrt{2}\,\Delta}\right) \Gamma\left(1 + \frac{1}{2}\, T\right) \quad , \tag{5.13}$$

where the Gamma function $\Gamma(1 + (1/2)T)$ can be approximated by $\Gamma(1 + (1/2)T) = 1 - (1/2)\, 0.5772157T$. T is defined by

$$T = \frac{2\alpha}{\pi} \left(\ell n\, \frac{s}{m_e^2} - 1\right) \Pi^{-1}\, \ell n(1 - \Pi)^{-1} \tag{5.14}$$

and its numerical value is tabulated in Table III. Equations (5.13) and (5.12) can be used to calculate the maximum counting rate. In general the beam energy resolution Δ is not known accurately enough, so it is not desirable to use the measurement at the peak to obtain $\Gamma(R \to e^+e^-)$, Γ_t, and $\Gamma(R \to f)$. The area method to be described below is independent of the machine width Δ, so it should be used to determine $\Gamma(R \to e^+e^-)$ and Γ_t. After this is done, one can then sit on top of the resonance peak and measure all other partial widths using (5.12) and (5.13) by comparing the final state of interest with the leptonic mode.

2. Area Method

The shape of the curve on the left hand side of the peak in Fig. 6 represents mainly the machine width whereas the shape of the curve on the right hand side and

far away from the peak is due to $1/k$ dependence of the radiative tail. If we integrate the experimental curve from W_{min} to W_{max} as shown in Fig. 6, we expect the area of the integration to become independent of the details of the machine width as long as $W_{max} - M_R$ is chosen to be much larger than the machine width. This situation is exactly the same as the treatment of scattering of an electron from a proton near the elastic peak (Tsai, 1961). Since the area becomes independent of the machine width we may replace $G(W, W')$ by a δ function

$$G(W, W') = \delta(W - W') \quad . \tag{5.15}$$

We obtain then from (5.12) and (5.10)

$$\begin{aligned} \int_{W_{min}}^{W_{max}} \sigma_{exp}(W) dW = \left(\frac{W_{max} - M_R}{(1/2)\, M_R}\right)^T \left[1 - \Pi(M_R^2)\right]^{-\delta^e_{vert}(M_R^2)/\Pi(M_R^2)} \\ \times \left[\frac{6\pi^2\, \Gamma(R \to e^+e^-)\, \Gamma(R \to f)}{\Gamma_t\, M_R^2}\right] \quad . \end{aligned} \tag{5.16}$$

W_{max} should be chosen so that $M_R \gg W_{max} - M_R \gg$ beam energy spread. In practice $W_{max} - M_R \geq (10 \text{ to } 15)\Delta$ will give a sufficiently accurate result.

The procedure for extracting various widths is as follows:

Step 1. $\Gamma(R \to e^+e^-)$ can be determined by the experiment $e^+e^- \to R \to$ all, because in this case $\Gamma(R \to f)$ and Γ_t in (5.16) cancel each other.

Step 2. Γ_t is then determined by the experiment $e^+e^- \to R \to e^+e^-$ which is proportional to $[\Gamma(R \to e^+e^-)]^2/\Gamma_t$.

Step 3. After $\Gamma(R \to e^+e^-)$ and Γ_t are determined using the area method, other decay modes can be investigated by operating the machine on the resonance peak where the maximum counting rate occurs. Other partial decay widths are determined then by comparing them with the leptonic width.

Had we used the lowest order leptonic width $\Gamma_0(R \to e^+e^-)$ instead of the experimental leptonic width, some confusion can occur in Step 2 and Step 3, because in Step 2 when the final state is e^+e^- the partial width $\Gamma(R \to f)$ in (5.16) should be written as $\Gamma_0(R \to e^+e^-)(1 - \Pi)^{-2}$ and in Step 3 the leptonic mode we are comparing with is the experimental one and not $\Gamma_0(R \to e^+e^-)$. This is why it is a good idea to use $\Gamma_{exp}(R \to e^+e^-)$ instead of $\Gamma_0(R \to e^+e^-)$. One can convert $\Gamma_{exp}(R \to e^+e^-)$ into

$\Gamma_0(R \to e^+e^-)$ by multiplying a factor $(1-\Pi)^2$ before doing a theoretical analysis, for example when obtaining the wave function of quarkonium at the origin etc.

In the next section we treat the case where the machine width is much narrower than the decay width using $e^+e^- \to Z_0 \to f$ as an example. Of course the method can be used also for the hadronic resonances.

VI. RADIATIVE CORRECTIONS TO $e^+e^- \to Z_0 \to f$

Since no photon intermediate state is necessary for the decay $Z_0 \to e^+e^-$, we should not include the vacuum polarization in the lowest order radiative corrections. Our formulae (5.8) and (5.9) can thus be used for the analysis of $e^+e^- \to Z_0 \to f$. The width of the Z_0 (see Cheng, 1982) according to the standard model is expected to be about 3 GeV which is much wider than the beam energy width (~ 0.1 GeV). If we approximate $G(W, W')$ by $\delta(W - W')$, then (5.9) can be written as

$$\begin{aligned}\sigma_{exp}(W) &= \int_0^W dW'' \, B(W, W'') \, \sigma_{eff}(W'') \\ &= \int_0^W T\left(\frac{2}{W}\right)^T \frac{1}{(W-W'')^{1-T}} \left[1 - \Pi(W''^2)\right]^{-\delta^e_{vert}(W''^2)/\Pi(W''^2)} \\ &\quad \times 12\pi \, \frac{\Gamma(Z_0 \to e^+e^-)\, \Gamma(Z_0 \to f)}{(W''^2 - M_Z^2)^2 + \Gamma_t^2 \, M_Z^2} \, dW'' \quad .\end{aligned} \tag{6.1}$$

Now T, Π and δ^e_{vert} are all slowly varying functions of W'', so we may evaluate them at the resonance peak $W'' = M_Z$. Using $M_z = (93.8 \pm 2.0)$ GeV (see Marciano, 1980) we obtain $\delta^e_{vert} = 0.087$, $\Pi = 0.061$ and $T = 0.111$ from Table III. Thus

$$(1-\Pi)^{-\delta^e_{vert}/\Pi} = 1.094 \quad . \tag{6.2}$$

Let us write

$$\sigma_{exp}(W)/\sigma_b(M_z) = BWR(W) \quad , \tag{6.3}$$

where $\sigma_b(M_z)$ is the peak value of Breit-Wigner cross section

$$\sigma_b(M_z) \equiv \left[12\pi \, \Gamma(Z_0 \to e^+e^-)\, \Gamma(Z_0 \to f) \, M_z^{-2} \, \Gamma_t^{-2}\right] \quad , \tag{6.4}$$

we have

$$BWR(W) \equiv 1.094\ M_z^2\ \Gamma_t^2 \int_0^2 \frac{Tx^{T-1}\,dx}{D^2 + M_z^2\ \Gamma_t^2} \tag{6.5}$$

with $D = W^2[1-(1/2)x]^2 - M_z^2$. $\sigma_b(M_z)$ is the peak value of the cross section at $W = M_z$ if there were no radiative corrections. *BWR* stands for Breit-Wigner radiatively corrected. In order to see the effect of radiative corrections to the resonance peak we have plotted in Fig. 7 $BWR(W)$ together with the original Breit-Wigner function $BW(W)$ which is defined by

$$BW(W) = \frac{\Gamma_t^2\ M_z^2}{(W^2 - M_z^2)^2 + \Gamma_t^2\ M_z^2} = \frac{\sigma_b(W)}{\sigma_b(M_z)} \quad . \tag{6.6}$$

The integrand in $BWR(W)$ defined by (6.5) is too singular to be evaluated reliably by a computer. This singularity can be eliminated by integration by parts:

$$BWR(W) = 1.094\ M_z^2\ \Gamma_t^2 \left[\frac{2^T}{M_z^4 + \Gamma_t^2\ M_z^2} + \int_0^2 \frac{2x^T\ DW^2[(1/2)x - 1]\ dx}{(D^2 + \Gamma_t^2\ M_z^2)^2}\right] \quad . \tag{6.5'}$$

In Fig. 7 we plot $BW(W)$ and $BWR(W)$. The figure shows that the originally symmetric Breit-Wigner function $BW(W)$ acquires a radiative tail toward the high energy side. The shift in peak position is only about 0.1 GeV. The peak height is reduced by about 24% and the width is increased by about 15%. In Table IV, we tabulate the shift in peak position $W_{peak} - M_z$, the ratio of the experimental peak height to the peak height of the Breit-Wigner $\sigma_{exp}(W_{peak})/\sigma_b(M_z)$, and the ratio of experimental full width at half maximum to Γ_t. The energies at half maximum is defined by $\sigma_{exp}(W_{\pm 1/2}) = (1/2)\sigma_{exp}(W_{peak})$. Each flavor of massless neutrino contribute to a partial width:

$$\Gamma(Z_0 \to \nu_f\, \bar{\nu}_f) = 2.2 \times (M_z \text{ in GeV})^3 \times 10^{-7}\ \text{GeV} \quad . \tag{6.7}$$

For M_z value of 93.8 GeV, this gives

$$\Gamma(Z_0 \to \nu_f\, \bar{\nu}_f) = 0.18\ \text{GeV} \quad . \tag{6.8}$$

The values of Γ_t used in Table IV correspond to different number of massless neutrinos participating in the decay of Z_0.

Table IV shows that the shift of the peak position increases slightly with Γ_t, it increases from 0.1 to 0.2 GeV as Γ_t is increased from 3 GeV to 3.54 GeV. The ratio $\sigma_{exp}(W_{peak})/\sigma_0(M_z)$ also increases slightly from .76 to .77, and the ratio of experimental width to Γ_t also increases slightly with the increase of Γ_t. The important thing to remember is that these correction can be calculated very reliably and thus M_z, Γ_t and $\Gamma(Z_0 \to e^+e^-)\,\Gamma(Z_0 \to f)/\Gamma_t^2$ can be determined from the experiment. Once Γ_t and M_z are determined the machine can then be set at W_{peak} and the partial widths of all the visible modes are then determined. The experimental cross section at the peak represents the product of quantities given in (6.4) times a calculable number ($\sim$ .76 $\sim$ .77) tabulated in Table V. After the sum of widths of all visible modes are measured, the number of flavors (N) of neutrino can then be obtained from $\Gamma_t - \Gamma_{visible} = N\Gamma(Z \to \nu_f \bar{\nu}_f)$, where $\Gamma(Z \to \nu_f \bar{\nu}_f)$ is given by (6.7). In order to simplify the treatment we have ignored the nonresonant background caused by one photon exchange near Z_0 pole. This interference effect is treated in detail by Greco, Pancheri-Srivastava and Srivastava (Greco, 1980) and by Berends, Kleiss and Jadach (Berends, 1982). The interference between the γ exchange and the Z_0 exchange diagrams is important only when the energy is far from the Z_0 pole. However, when the energy is far from the Z_0 pole other higher order electroweak diagrams besides the QED corrections to the lowest order diagrams become important. These higher order (α^3) electroweak diagrams have been considered by Passarino and Veltman (Passarino, 1979). It would be very interesting to see whether one can identify the effects of these higher order electroweak graphs experimentally by investigating the energy dependence of the cross sections for processes such as $e^+e^- \to \mu^+\mu^-$. Some theoretically trivial but numerically significant improvements must be made on Passarino and Veltman's work before it can be used by experimenters: 1. The width of Z_0 should not be ignored; 2. The photon spectrum should be modified from $x^{-1}dx$ to $(1+(1-x)^2)/(2x^{1-T})dx$, see Eq. (4.1), in order to take care of both soft and hard photon regions; 3. τ and hadron contricutions should be added to their vacuum polarization diagrams.

VII. CONCLUSION AND SUMMARY

Using the renormalization group technique we obtained all the leading log terms to all order in α using the results from the lowest order radiative corrections. We point

out in the Appendix that this can be derived without assuming that the limit $m^2 \to 0$ exists. We have restored the mass dependence of the logarithmic terms by judiciously changing the results of the renormalization group technique. This renders the result usable in practical calculations.

ACKNOWLEDGEMENTS

The author wishes to thank Mike Levi and Harvey Lynch for many hours of discussion on this subject. The author also benefited greatly from discussions with Drs. Ming Chen, G. Passarino, M. Peskin, Y. P. Yao and D. R. Yennie.

APPENDIX A: Renormalization Group in QED

In quantum electrodynamics, because of the gauge invariance, the mass renormalization and the wave function renormalization cancel ($Z_1 = Z_2$) each other, hence only the charge renormalization needs to be considered. The renormalization group in QED is simply a statement that "physics" should be independent of the value of momentum transfer at which we renormalize the charge. It is truly remarkable that such a simple and seemingly obvious statement can yield so many nontrivial results. In the above by "physics" we mean any quantity which is a function of charge, such as vacuum polarization, vertex function, cross section, asymmetry, etc. The vacuum polarization plays a central role in this scheme because it defines the charge e_λ^2 corresponding to different renormalization point λ. Let us first consider the vacuum polarization $d(q^2/\lambda^2,\ m^2/\lambda^2,\ e_\lambda^2)$ where λ^2 is the value of q^2 at which the charge e_λ^2 is defined:

$$d(1,\ m^2/\lambda^2,\ e_\lambda^2) = e_\lambda^2 \quad . \tag{A.1}$$

The basic supposition of the renormalization group is that $d(q^2/\lambda^2,\ m^2/\lambda^2,\ e_\lambda^2)$ is independent of λ, therefore

$$d(q^2/\lambda^2,\ m^2/\lambda^2,\ e_\lambda^2) = d(q^2/\lambda_1^2,\ m^2/\lambda_1^2,\ e_{\lambda_1}^2) \quad . \tag{A.2}$$

We want to solve for $d(q^2/\lambda_1^2,\ m^2/\lambda_1^2,\ e_{\lambda_1}^2)$ using (A.1) and (A.2). In order to do this we define $x = q^2/\lambda^2$, $y = m^2/\lambda^2$ and $t = \lambda_1^2/\lambda^2$, so (A.2) becomes

$$d(x,\ y,\ e_\lambda^2) = d(x/t,\ y/t,\ d(t, y, e_\lambda^2)) \quad , \tag{A.3}$$

where we have written $e_{\lambda_1}^2 = d(t, y, e_\lambda^2)$ which can be obtained by letting $q^2 = \lambda_1^2$ in (A.2). Since t is arbitrary in (A.3), we may differentiate (A.3) with respect to x and then let $t = x$. This yields

$$\begin{aligned} \frac{\partial}{\partial x}\, d(x, y, e_\lambda^2) &= \frac{1}{x}\left[\frac{d}{d\xi}\, d(\xi,\ y/x,\ d(x, y, e_\lambda^2))\right]_{\xi=1} \\ &\equiv \frac{1}{x}\,\Phi\Big(y/x,\ d(x, y, e_\lambda^2)\Big) \quad . \end{aligned} \tag{A.4}$$

The solution to (A.4) can be written formally as

$$\ell n\, x = \int_{e_\lambda^2}^{d(x,y,e_\lambda^2)} \frac{d[d(x, y, e_\lambda^2)]}{\Phi(y/x,\ d(x, y, e_\lambda^2))} \quad . \tag{A.5}$$

(A.5) is still exact. What we want to do is to use it to obtain a better expression for $d(x, y, e_\lambda^2)$ using the perturbation theory calculation up to one loop for $\Phi(y/x, d(x, y, e_\lambda^2))$. The perturbation results for the unrenormalized d up to e^4 for a pair of fermions with mass m in the loop was given by Feynman (Feynman, 1949):

$$d_{unr}(q^2,\ \Lambda^2,\ e^2) = e^2\left[1+\frac{e^2}{4\pi^2}\left(-\frac{1}{3}\ \ell n\ \frac{\Lambda^2}{m^2}+\left\{-\frac{4m^2+2q^2}{3q^2}\left(1-\frac{a}{\tan a}\right)+\frac{1}{9}\right\}\right)\right]\ , \quad (A.6)$$

where e^2 is the unrenormalized change, Λ is the cut off parameter, a is a complex number given by $q^2 = 4m^2\ \sin^2 a$. The real part of terms inside the curly bracket in (A.6) is equal to the function $f(x)$ in (2.7) and (2.8). When $q^2 > 4m^2$ there is a positive imaginary part coming from $a = \pi/2 + iu$ where $\sinh\ u = +(q^2/4m^2 - 1)^{1/2}$ and $-1/\tan\ a = i\tanh\ u = +i(q^2 - 4m^2)^{1/2}\ (q^2)^{-1/2}$. This imaginary part can be obtained also from (2.6) by using the identity $(s-s'-i\epsilon)^{-1} = P(s-s')^{-1} + i\pi\delta(s-s')$. From (A.6) we can write down immediately the expression for $d_r(q^2, \lambda^2, e_\lambda^2)$, which is renormalized at $q^2 = \lambda^2$ for any value of λ^2:

$$\begin{aligned} d_r(q^2, \lambda^2, e_\lambda^2) = & e_\lambda^2\left[1+\frac{e_\lambda^2}{4\pi^2}\left[\left\{-\frac{4m^2+2q^2}{3q^2}\left(1-\frac{a}{\tan a}\right)+\frac{1}{9}\right\}\right.\right. \\ & \left.\left. -\left\{-\frac{4m^2+2\lambda^2}{3\lambda^2}\left(1-\frac{a_\lambda}{\tan a_\lambda}\right)+\frac{1}{9}\right\}\right]\right] \end{aligned} \quad (A.7)$$

where a_λ is related to λ by $\lambda^2 = 4m^2\ \sin^2 a_\lambda$. In order to avoid confusion we use $d_r(q^2, \lambda^2, e_\lambda^2)$ to represent $d(q^2/\lambda^2, m^2/\lambda^2, e_\lambda^2)$ which is awkward when $\lambda^2 = 0$. Equation (A.7) is too complicated to be used for the integration shown in (A.5). At high energies $|q^2| \gg m^2$, the first curly bracket in (A.7) becomes $(1/3)\ell n(-q^2/m^2) - (5/9)$. The second curly bracket is $(1/3)\ell n(-\lambda^2/m^2) - (5/9)$ if $|\lambda^2| \gg m^2$, and when $|\lambda^2| \ll m^2$ it is $-\lambda^2/15m^2$. We have thus

$$d_r(q^2,\ 0,\ e_0^2) \underset{|q^2|\gg m^2}{\rightarrow} e_0^2\left[1+\frac{e_0^2}{4\pi^2}\left(\frac{1}{3}\ \ell n\left(-\frac{q^2}{m^2}\right)-\frac{5}{9}\right)\right] \quad (A.8)$$

and

$$d_r(q^2,\ \lambda^2,\ e_\lambda^2) \underset{\substack{|\lambda^2|\gg m^2 \\ |q^2|\gg m^2}}{\rightarrow} e_\lambda^2\left[1+\frac{e_\lambda^2}{4\pi^2}\ \frac{1}{3}\ \ell n\ \frac{q^2}{\lambda^2}\right]\ . \quad (A.9)$$

Now the condition $|\lambda^2| \gg m^2$ can be relaxed for the validity of Eq. (A.9) because even when $|\lambda^2| = m^2$ (A.9) is still a good approximation. When $\lambda^2 = m^2$ the second curly bracket in (A.7) is -0.0751 which is small compared with $(1/3)\ell n(q^2/m^2)$ coming from the first curly bracket. We also note (A.9) is valid when $q^2 = \lambda^2$ as long as $|q^2| \gg m^2$. From the basic supposition of renormalization group, $d_r(q^2, 0, e_0^2) = d_r(q^2, \lambda^2, e_\lambda^2)$. Hence letting $q^2 = \lambda^2$ in both sides of (A.8) and (A.9) we obtain

$$e_\lambda^2 \underset{\substack{|q^2|\gg m^2 \\ |\lambda^2|\geq m^2}}{=} e_0^2 \left[1 + \frac{e_0^2}{4\pi^2}\left(\frac{1}{3}\,\ell n\left(-\frac{\lambda^2}{m^2}\right) - \frac{5}{9}\right)\right] \quad . \tag{A.10}$$

This shows that the mass singularity appearing in (A.8) becomes the mass singularity in e_λ^2 and (A.9) is now free from mass singularity except in the definition of e_λ^2. Thus in the limits $|q^2| \gg m^2$ and $|\lambda^2| \geq m^2$ the functions d and Φ in (A.4) and (A.5) are free from y dependence, all the mass dependence is contained in the definition of e_λ^2. Φ in (A.5) is now function of $d(x, y, e_\lambda^2)$ alone and $d(x, y, e_\lambda^2)$ is the variable of integration. From (A.9) we have

$$\Phi\left(\frac{y}{x}\,,\; z\right) = \frac{z^2}{12\pi^2} \quad . \tag{A.11}$$

Substituting (A.10) into (A.5) we obtain

$$\ell n\; x = 12\pi^2\left(\frac{1}{e_\lambda^2} - \frac{1}{d(x, y, e_\lambda^2)}\right)$$

which gives

$$d(x, y, e_\lambda^2) = \frac{e_\lambda^2}{1 - (e_\lambda^2/12\pi^2)\;\ell n\; x} \quad . \tag{A.12}$$

We can recover all the mass dependence of d by substituting the expression for e_λ^2 given by (A.10) into (A.12),

$$d_r(q^2,\; 0,\; e_0^2) = \frac{e_0^2}{\left[1 + \frac{e_0^2}{4\pi^2}\left(\frac{1}{3}\;\ell n\; -\frac{\lambda^2}{m^2} - \frac{5}{9}\right)\right]^{-1} - \frac{e_0^2}{12\pi^2}\;\ell n\;\frac{q^2}{\lambda^2}} \tag{A.13}$$

$$\approx \frac{e_0^2}{1 - \frac{e_0^2}{4\pi^2}\left(\frac{1}{3}\;\ell n\; -\frac{q^2}{m^2} - \frac{5}{9}\right)} \quad . \tag{A.14}$$

We have made an approximation to obtain (A.14) from (A.13), but (A.14) makes more sense than (A.13) because it is just a summation of chain diagrams for the vacuum polarization. We have assumed that only one kind of fermion pair contributes to the vacuum polarization. We can prove easily that the method can be extended to the actual case where many different particles participates in the vacuum-polarization. In actual calculations we shall use the form

$$d_r(q^2,\ 0,\ e_0^2) = \frac{e_0^2}{1-\Pi(q^2)} \tag{A.15}$$

where $\Pi(q^2)$ is the lowest order vacuum polarization including all particles (e, μ, τ, hadrons) as defined in (2.5) and (2.6), even though the condition $|q^2| \gg m^2$ may not be satisfied for some of the particles. The reason is that (A.15) can be obtained by summing the chain graphs i.e., $1+\Pi+\Pi^2+\ldots = 1/(1-\Pi)$, which does not require that $|q^2| \gg m^2$ is satisfied. We might ask what have we gained by using the renormalization group to obtain (A.15) if it can be obtained using another method? We shall show in the following that the chain sum of the lowest order vacuum polarization diagrams contains all the leading logs in perturbation series. By leading logs we mean terms of order $\alpha^n\, \ell n^n(q^2/m^2)$ in Π. A term such as $\alpha^n\, \ell n^{n-1}(q^2/m^2)$ is not a leading log.

In order to demonstrate this let us suppose that we have calculated $d(q^2, \lambda^2, e_\lambda^2)$ to all orders

$$d(x,\ y,\ e_\lambda^2) = e_\lambda^2 \left[1 + \sum_{\substack{n\geq 1 \\ n\geq \ell \geq 0}} a_{n\ell} (e_\lambda^2)^n\ (\ell n\, x)^\ell\right] \quad . \tag{A.16}$$

We can then calculate

$$\begin{aligned} \Phi\left(\frac{y}{x}\ ,\ z\right) &= \left[\frac{\partial}{\partial \xi}\ d(\xi,\ y,\ z)\right]_{\xi=1} \\ &= z\left(\sum_{n\geq 1}\ a_{n1}\ z^n\right) \quad . \end{aligned} \tag{A.17}$$

Apparently only terms linear in $\ell n\, x$ contribute to Φ. This is the most profound statement. It means that the high energy behavior of $d_r(q^2, \lambda^2, e_\lambda^2)$ is completely determined by the coefficients of terms linear in $\ell n\, x$, specifically the coefficients a_{n1} from $n = 1, \ldots, k$ will determine all the coefficients $a_{\ell,\ell}$, $a_{\ell+1,\ell}$, $a_{\ell+2,\ell}$, $\ldots$, $a_{\ell+k-1,\ell}$

for all $\ell = 1, \ldots, \infty$. In other words, if we want to know the leading log terms to all orders, we need to calculate only a_{11}, if we want to know terms next to the leading logs to all orders then we need to calculate only a_{11} and a_{21} etc. In order to prove this all we need to show is that a_{k1} will not contribute to $a_{\ell+k',\ell}$ for $k' < k-1$, and $\ell = 1, 2, \ldots, \infty$. Let us assume that we know the coefficients $a_{11}, a_{21}, \ldots, a_{k1}$. From Eqs. (A.5) and (A.17) we obtain

$$\ell n\ x = \int_{e_\lambda^2}^{d(x,y,e_\lambda^2)} \frac{dz}{z^2[a_{11} + a_{21}z + \ldots + a_{k1}z^{k-1}]} \quad . \tag{A.18}$$

Now $d(x, y, e_\lambda^2)$ does not differ greatly from e_λ^2 and also we may assume that the quantity inside [ ] does not vary greatly in the interval of integration. Thus we may pull the factor [ ] out of the integral and replace z by η which lies somewhere between e_λ^2 and $d(x, y, e_\lambda^2)$. The integration can then be carried out and we obtain

$$\begin{aligned} d(x,\ y,\ e_\lambda^2) &= \frac{e_\lambda^2}{1 - e_\lambda^2\, \ell n\, x[a_{11} + a_{21}\eta + a_{31}\eta^2 + \ldots + a_{k1}\eta^{k-1}]} \\ &= e_\lambda^2 \left[1 + e_\lambda^2\, \ell n\, x[\ldots] + (e_\lambda^2\, \ell n\, x)^2[\ldots]^2 + \ldots + (e_\lambda^2\, \ell n\, x)^\ell[\ldots]^\ell + \ldots\right] \end{aligned} \tag{A.19}$$

where $[\ldots]$ represents the terms inside the square bracket. Let us consider the term $[\ldots]^\ell$. The minimum power of e_λ^2 associated with a_{k1} in $[a_{11} + a_{21}\eta + a_{31}\eta^2 + \ldots + a_{k1}\eta^{k-1}]^\ell$ is $k-1$. Thus a_{k1} can contribute to $a_{\ell+k-1,\ell}$ but not to $a_{\ell+k-2,\ell}$, $a_{\ell+k-3,\ell}$, $\ldots, a_{\ell,\ell}$. This proves the observation first made by Perrin (Perrin, 1966), who used a more ellaborate method to prove this point. The most important corollary of this point is that the higher order irreducible graphs do not contribute to the leading logs of the vacuum polarization because they are all given by the chain summation of the one loop graphs.

Let us next consider other physical quantities which contain charges, for example a vertex function or a cross section. Let us denote this by $F(q^2/\lambda^2,\ m_1^2/\lambda^2,\ e_\lambda^2)$. In general the mass (or masses occuring in F may not be the same as the one occuring in d). From the fact that $F(q^2/\lambda^2,\ m_1^2/\lambda^2,\ e_\lambda^2)$ is independent of choice of λ, we obtain

$$F(x,\ y,\ e_\lambda^2) = F\left(\frac{x}{t}\ ,\ \frac{y}{t}\ ,\ d(t, e_\lambda^2)\right) \quad . \tag{A.20}$$

We have used the fact that in the high energy limit m dependence of d function is all absorbed in e_λ^2. Taking the logarithmic derivative of (A.20) with respect to x and then setting $t = x$ we obtain

$$\frac{\partial}{\partial x}\ \ell n\ F(x,y,e_\lambda^2) = \frac{1}{x}\ \psi\left(\frac{y}{x}\ ,\ d(x,e_\lambda^2)\right) \tag{A.21}$$

where

$$\psi(y,e_\lambda^2) = \left[\frac{\partial}{\partial \xi}\ \ell n\ F(\xi,y,e_\lambda^2)\right]_{\xi=1} \quad . \tag{A.22}$$

Integrating (A.21) with respect to x from $x = 1$ to $x = x$ we obtain

$$\ell n\ \frac{F(x,y,e_\lambda^2)}{F(1,y,e_\lambda^2)} = \int_1^x \frac{dx}{x}\ \psi\left(\frac{y}{x}\ ,\ d(x,e_\lambda^2)\right) \quad . \tag{A.23}$$

Equation (A.23) is still exact. This equation is very profound. It says that function $F(x,y,e_\lambda^2)$ can be determined entirely once its logarithmic derivative at $x = 1$ is known. We calculate ψ up to one loop in perturbation theory and use Eq. (A.23) to improve the results. It can be shown that the results contain leading log terms of all orders in α.

Let the result of one loop calculation at high energy be

$$\begin{aligned} F_1(x,y,e_\lambda^2) &= 1 + e_0^2(a_F + C_F\ \ell n(q^2/m^2)) \\ &= 1 + e_0^2(a_F + C_F\ \ell n\, x - C_F\ \ell n\, y) \end{aligned} \tag{A.24}$$

where a_F and C_F are quantities independent of e_0^2 and q^2. e_0^2 is related to e_λ^2 by (A.10) hence to the order we want e_0^2 is equal to e_λ^2. From (A.22) and (A.24) we obtain to order e_λ^2:

$$\psi(y,\ e_\lambda^2) = e_\lambda^2\ C_F \quad , \tag{A.25}$$

which is independent of y. We have therefore

$$\psi\left(\frac{y}{x}\ , d(x,e_\lambda^2)\right) = C_F\ d(x,\ e_\lambda^2) \quad . \tag{A.26}$$

Substituting

$$d(x,\ e_\lambda^2) = \frac{e_\lambda^2}{1 - e_\lambda^2\ C_\Pi\ \ell n\, x} \tag{A.27}$$

into (A.26) and performing the integration in (A.23), we obtain

$$\ell n \frac{F(x,\ y,\ e_\lambda^2)}{F(1,\ y,\ e_\lambda^2)} = \frac{C_F}{C_\Pi}\ \ell n \left(\frac{1}{1 - e_\lambda^2\ C_\Pi\ \ell n\, x}\right) \quad ,$$

which yields

$$F(x,\ y,\ e_\lambda^2) = F(1,\ y,\ e_\lambda^2) \left(\frac{1}{1 - e_\lambda^2\ C_\Pi\ \ell n\, x}\right)^{C_F/C_\Pi} \quad . \tag{A.28}$$

This is the relation derived by Erikkson. We went through the derivation in detail in order to show that it is not necessary to assume that the functions d and F are finite in the limit $m^2 \to 0$ for derivation of the result. From the perturbation results we know both d and F diverge in the limit $m^2 \to 0$. Since this is a bonafide physical property it cannot be eliminated by the choice of λ (it would be against the basic supposition of the renormalization group if it can). The apparent independence of d on m^2 in Eq. (A.12) is because all the m^2 dependence of d is hidden in the definition of e_λ^2:

$$e_\lambda^2 = \frac{e_0^2}{1 - (e_0^2/12\pi^2)\ \ell n(\lambda^2/m^2)} \quad . \tag{A.29}$$

λ^2 in (A.28) is arbitrary. We may conveniently choose $\lambda^2 = m^2$, then in the high energy limit $e_\lambda^2 = e_0^2$ and of course $y = 1$. In QED the mass singularity occur in the form $\ell n(q^2/m^2) = \ell n\, x - \ell n\, y$. Thus when $x = y = 1$ all the log terms disappear. The term $F(1, y, e_\lambda^2)$ in (A.28) can therefore be approximated by the nonlogarithmic term of the one loop calculation, the higher order terms being negligible. In Eq. (2.3) which is our proposed improved formula for (A.28), the expression A contains the logarithmic as well as nonlogarithmic terms from one loop radiative corrections. Thus the factor $F(1, y, e_\lambda^2)$ is dropped to avoid double counting of nonlog terms.

It is important to notice that there are no double log terms such as $\ell n^2(s/m^2)$, $\ell n^2(u/m^2)$ and $\ell n^2(t/m^2)$ in Eq. (A.24). These double log terms occur in the bremsstrahlung diagrams, vertex functions and the two photon exchange diagrams when the photon mass λ is used as the infrared cut off. As shown by Tsai (Tsai 1960, 1961) these double logs always occur in the form:

$$K(p_i,\ p_j) = (p_i \cdot p_j) \int_0^1 \frac{dy}{p_y^2}\ \ell n(p_y^2/\lambda^2) \quad , \tag{A.30}$$

where $p_y = p_i y + (1-y)p_j$ and p_i and p_j are momenta of two external particles from which an infrared photon (real or virtual) is emitted. This term occurs with an opposite sign in real and virtual photon emissions and thus will not appear in the cross section. Each term in the expression of A given by Eq. (2.4) represents the remainder after the functions $K(p_i, p_j)$'s are subtracted. For example, the electron vertex part contains $K(p_1, p_1)$, $K(p_2, p_2)$ and $K(p_1, p_2)$. The expression $\delta^e_{vert}(s)$ given in Eq. (2.4) represents the electron vertex function after these three infrared functions have been subtracted. Similarly the bremsstrahlung from the e^+e^- llines contain $K(p_1, p_1)$, $K(p_2, p_2)$ and $K(p_1, p_2)$, each with an opposite sign from the corresponding one in the electron vertex function. The expression $-t_e \ell n E/\Delta E$ in Eq. (2.4) represents the bremsstrahlung from the initial electron-positron line after these infrared functions have been subtracted. The easiest way to see that these double log terms arise purely because the photon mass λ is used as the infrared cut off is to use the noncovariant infrared cut off for the real bremsstrahlung. The bremsstrahlung cross section from the e^+e^- is, for example,

$$\frac{2\alpha}{\pi}(\ell n(q^2/m_e^2) - 1) \int_{k_{min}}^{k_{max}} \frac{dk}{k}$$

which does not have a double log. Since we know the sum of bremsstrahlung cross section and the vertex function does not have double logs, we conclude that the vertex function should also not have double logs if we use the non-covariant soft photon cut off.

REFERENCES

Berends, F. A., and R. Gastmans, 1978, in *Electromagnetic Interactions of Hadrons*, Vol. 2, p. 471, edited by A. Donnachie and G. Shaw (Plenum Publishing Corporation).

Berends, F. A., R. Gastmans and T. T. Wu, 1979, KUL-TF-79/022, University of Leuven preprint.

Berends, F. A., and R. Kleiss, 1981, Nucl. Phys. B177, 237.

Berends, F. A., R. Kleiss and S. Jadach, 1982, Nucl. Phys. B22, 63.

Bjorken, J. D., 1963, Ann. Phys. (N.Y.) 24, 201.

Bloch, F., and A. Nordsieck, 1937, Phys. Rev. 52, 54.

Bogoliubov, N. N., and D. V. Shirkov, 1959, *Introduction to the Theory of Quantized Fields* (Interscience Publishers, Inc., New York).

Cheng, Ta-Pei, and Ling-Fong Li, 1982, *Gauge Theory of Elementary Particle Physics*, Carnegie-Mellon University Preprint.

Cabibbo, N., and R. Gatto, 1961, Phys. Rev. 124, 1577.

Eriksson, K. E., 1963, Nuovo Cimento 27, 178.

Eriksson, K. E., 1968, *Cargese Lectures in Physics*, ed. M. Lévy (Gordon and Beach, New York).

Feynman, R. P., 1949, Phys. Rev. 76, 769.

Gell-Mann, M., and F. Low, 1954, Phys. Rev. 95, 1300.

Greco, M., G. Pancheri-Srivatava and Y. Srivastava, 1980, Nucl. Phys. B171, 118 (E: B197 (1982) 543).

Jackson, J. D., and D. L. Scharre, 1975, Nucl. Instrum. Methods 128, 13.

Kinoshita, T., 1962, J. Math. Phys. 3, 650.

Kroll, N., and W. Wada, 1955, Phys. Rev. 98, 1355.

Lee, T. D., and M. Nauenberg, 1964, Phys. Rev. 133, B1549.

Marciano, W., and A. Sirlin, 1980, Phys. Rev. D22, 2695.

Mo, L. W., and Y. S. Tsai, 1964, Rev. Mod. Phys. 41, 205.

Pessarino, G., and M. Veltman, 1979, Nucl. Phys. B160, 151.

Perrin, R., 1966, *The Renormalization Group in Quantum Electrodynamics*, Harvard University preprint. This work was discussed in detail in Eriksson's article (Eriksson 1968).

Schwinger, J., 1949, Phys. Rev. 76, 790.

Stueckelberg, E. C. G., and A. Peterman, 1953, Helv. Phys. Acta 26, 499.

Tsai, Y. S., 1960, Phys. Rev. 120, 269.

Tsai, Y. S., 1961, Phys. Rev. 122, 1898.

Tsai, Y. S., 1965, in Proceedings of the International Symposium on Electron and Photon Interactions at High Energies, Hamburg (Deutsche Physikalische Gesellsdraft e.V.), Part II, p. 392.

Tsai, Y. S., 1971, *Radiative Corrections to Electron Scattering*, SLAC-PUB-848 (unpublished).

Tsai, Y. S., 1974, *Notes From the SLAC Theory Workshop on the ψ*, SLAC-PUB-1515 (unpublished).

Yennie, D. R., S. C. Frantschi and H. Suura, 1961, Ann. Phys. 13, 379.

Yennie, D. R., 1975, Phys. Rev. Lett. 34, 239.

Table I

Noninfrared and asymmetric part of the radiative correction $\delta_A(\theta) = -\delta_A(\pi - \theta)$. This function is independent of energy in the extreme relativistic limit. θ is defined as the angle between e^- and μ^-.

θ (degree)	δ_A (percent)
1	9.0
2	6.5
3	5.2
5	3.9
10	2.4
20	1.3
30	0.8
40	0.5
50	0.3
60	0.2
70	0.1
80	0.1
90	0

Table II

Resonances in e^+e^- annihilation and the parameters necessary to calculate $\delta_{vac}^{Res}(s)$ a la Eq. (2.14).

Resonance	M_R (MeV)	Γ_t (MeV)	Γ_{ee} (keV)	$6\Gamma(R \to ee)/\alpha M_R \times 10^3$
ρ	770	154	6.6	7.0
ω	783	9.9	0.7	0.73
ϕ	1020	4.21	1.3	1.05
ρ'	1600	300	?	?
J/ψ	3100	0.063	4.6	1.21
ψ'	3685	0.215	1.9	0.42
ψ''	3770	25	0.27	0.06
ψ'''	4030	52	0.73	0.14
ψ''''	4159	78	0.78	0.15
ψ'''''	4415	43	0.43	0.08
γ	9456	0.042	1.3	0.11
γ'	10020	0.030	0.51	0.04
γ''	10350	?	?	?

Table III

Various quantities needed for calculating the radiative corrections.

$\delta_s = \delta^e_{vert} + \delta^\mu_{vert} + \delta^e_{vac} + \delta^\mu_{vac} + \delta^\tau_{vac} + \delta^{had}_{vac}$.

All quantities are in percent.

$\sqrt{s}$ GeV	δ^e_{vert}	δ^μ_{vert}	δ^e_{vac}	δ^μ_{vac}	δ^τ_{vac}	δ^{had}_{vac}	δ_s	$\Pi = \delta_{vac}/2$	t_e	T
1	5.6	1.9	2.1	0.4	-0.0	0.5	10.4	1.5	6.58	6.63
3.1	6.4	2.7	2.4	0.8	-0.0	0.9	13.2	2.1	7.63	7.71
5	6.7	3.0	2.6	0.9	-0.1	1.9	15.0	2.7	8.08	8.18
10	7.2	3.5	2.8	1.2	0.2	2.7	17.6	3.5	8.72	8.87
20	7.7	4.0	3.0	1.4	0.5	3.8	20.3	4.4	9.37	9.57
29	7.9	4.2	3.1	1.5	0.6	4.3	21.7	4.8	9.71	9.94
34	8.0	4.3	3.2	1.5	0.7	4.6	22.3	5.0	9.86	10.1
50	8.3	4.6	3.3	1.7	0.8	5.1	23.7	5.5	10.2	10.5
100	8.8	5.1	3.5	1.9	1.0	6.0	26.3	6.2	10.9	11.2
200	9.3	5.6	3.7	2.1	1.2	7.0	28.8	7.0	11.5	11.9

Table IV

Effects of radiative corrections to the Z_0 peak for different values of Γ_t. $W_{peak} - M_z$ represents shift in peak energy, $\sigma_{exp}(W_{peak})/\sigma_b(M_z)$ represents the ratio of the experimental peak height to the peak height of the Breit-Wigner cross section, $(W_{+1/2} - W_{-1/2})/\Gamma_t$ represent the ratio of the experimental full width at half maximum to Γ_t. We assumed $M_z = 93.8$ GeV. The standard model gives $\Gamma_t = 3.0$ GeV. All these numbers are obtained numerically by computer using Eq. (6.5′).

	3ν's	4ν's	5ν's	6ν's
Γ_t (GeV)	3.0	3.18	3.36	3.54
$W_{peak} - M_z(93.8)$	0.1 GeV	0.15 GeV	0.2 GeV	0.2 GeV
$\sigma_{exp}(W_{peak})/\sigma_b(M_z)$	.76	.76	.77	.77
$(W_{+1/2} - W_{-1/2})/\Gamma_t$	1.143	1.145	1.155	1.167

FIGURE CAPTIONS

Fig. 1. Diagrammatic representation of the expansion $\delta^e_{vert}[1 + (1/2)\Pi + (1/3)\Pi^2 + \ldots]$.

Fig. 2. (a) Diagrams representing $[\delta^e_{vert}\ \Pi^{-1}\ \ell n(1-\Pi)^{-1}]^2/2!$.
(b) Diagrams representing $[\delta^e_{vert}\ \Pi^{-1}\ \ell n(1-\Pi)^{-1}]^3/3!$.
(c) Diagrams representing $[\delta^e_{vert}\ \Pi^{-1}\ \ell n(1-\Pi)^{-1}]^4/4!$.

Fig. 3. Diagrams associated with $t_e\ \ell n(E/\Delta E)[1 + (1/2)\Pi + (1/3)\Pi^2 + (1/4)\Pi^3 + \ldots]$.

Fig. 4. Diagrams associated with $[-t_e\ \ell n(E/\Delta E)\ \Pi^{-1}\ \ell n(1-\Pi)^{-1}]^2/2!$.

Fig. 5. Some of the diagrams associated with the α^4 cross section for (a) $e^+e^- \to \mu^+\mu^-$, (b) $e^+e^- \to \mu^+\mu^-\gamma$, (c) $e^+e^- \to \mu^+\mu^-\gamma\gamma$, and (d) $e^+e^- \to \mu^+\mu^-$ + pair. The diagrams containing the vacuum polarization in the main photon propagator as well as the diagrams containing multiple photon exchange between e and μ are omitted. In order to simplify the illustration, only one diagram among the gauge invariant subset of diagrams is shown.

Fig. 6. Schematic diagram of experimental cross section for the reaction $e^+e^- \to$ narrow resonance $\to$ final states.

Fig. 7. Effect of raditive corrections to the shape of the Breit-Wigner cross section for Z_0 peak assuming $M_z = 93.8$ GeV and $\Gamma_t = 3.0$ GeV. The solid curve represents the Breit-Wigner cross section normalized to unity at the peak. The dotted curve is the radiatively corrected cross section.

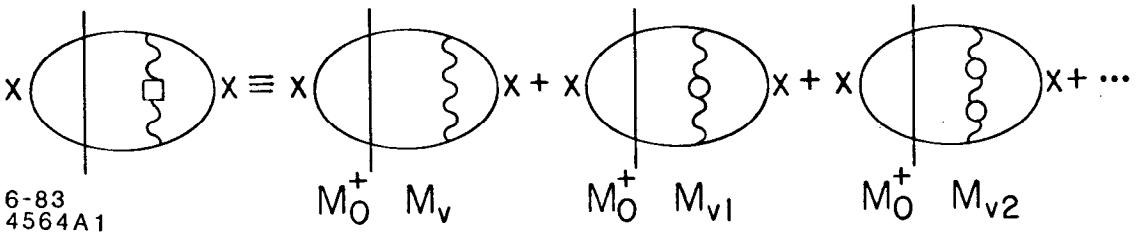

Fig. 1

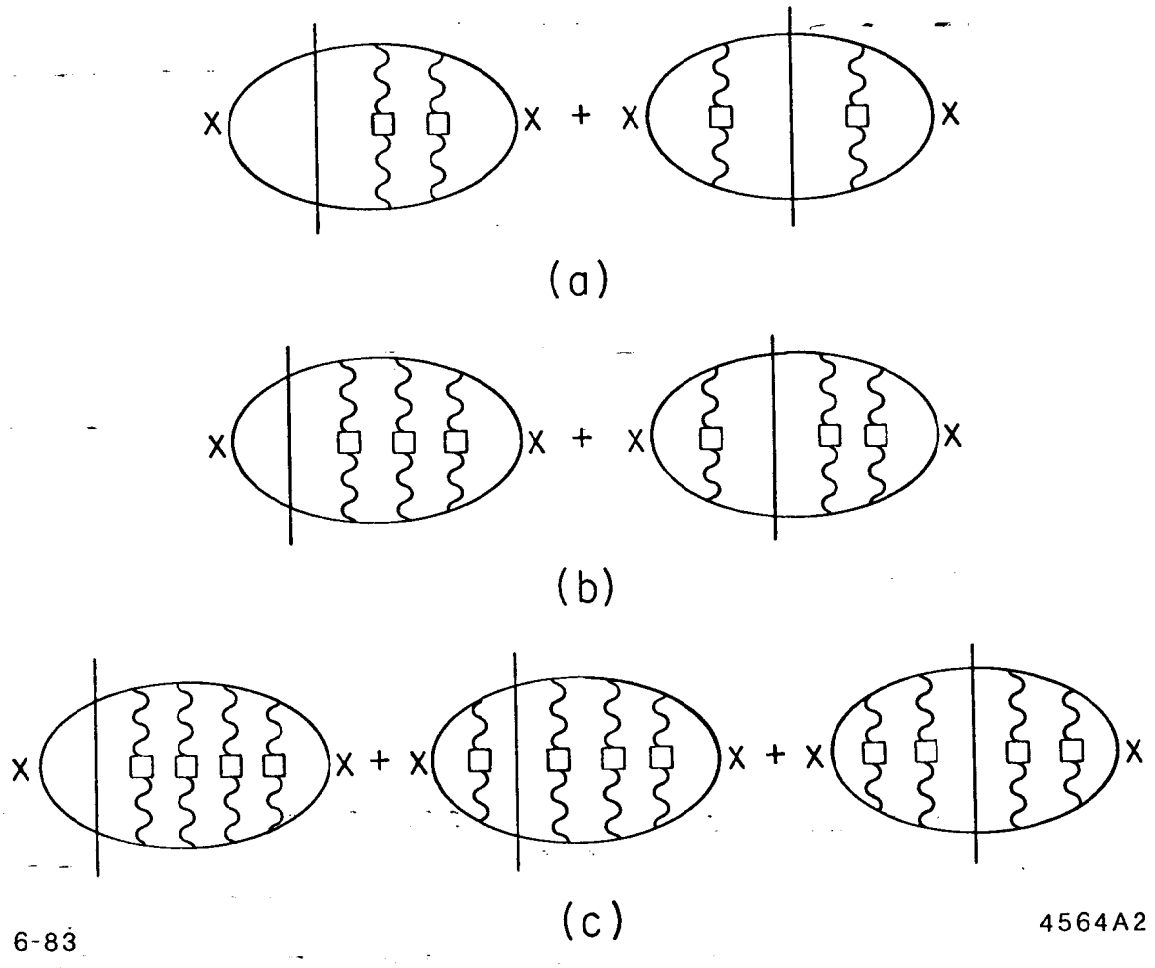

Fig. 2

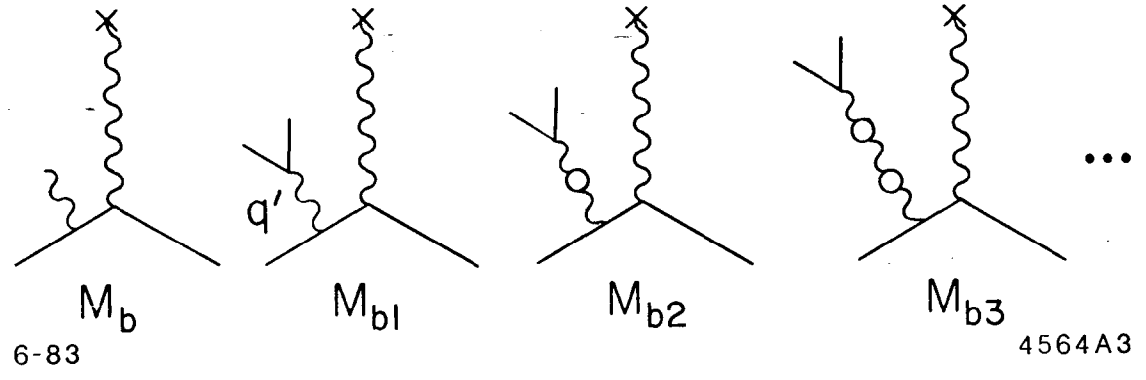

Fig. 3

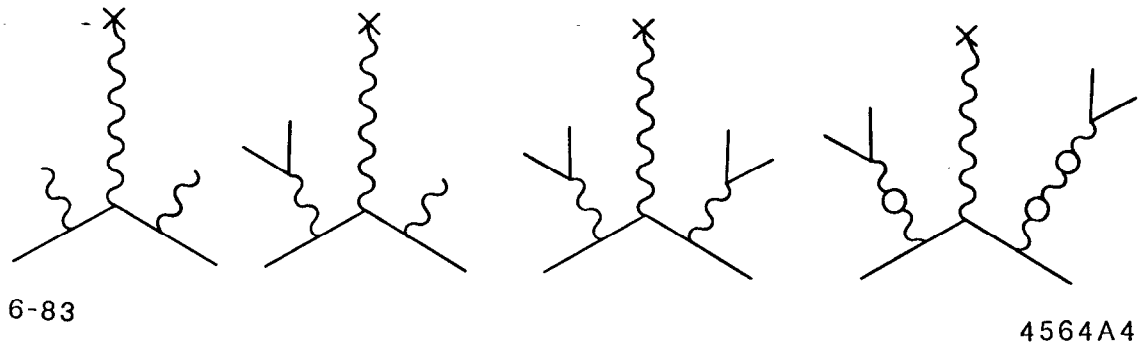

Fig. 4

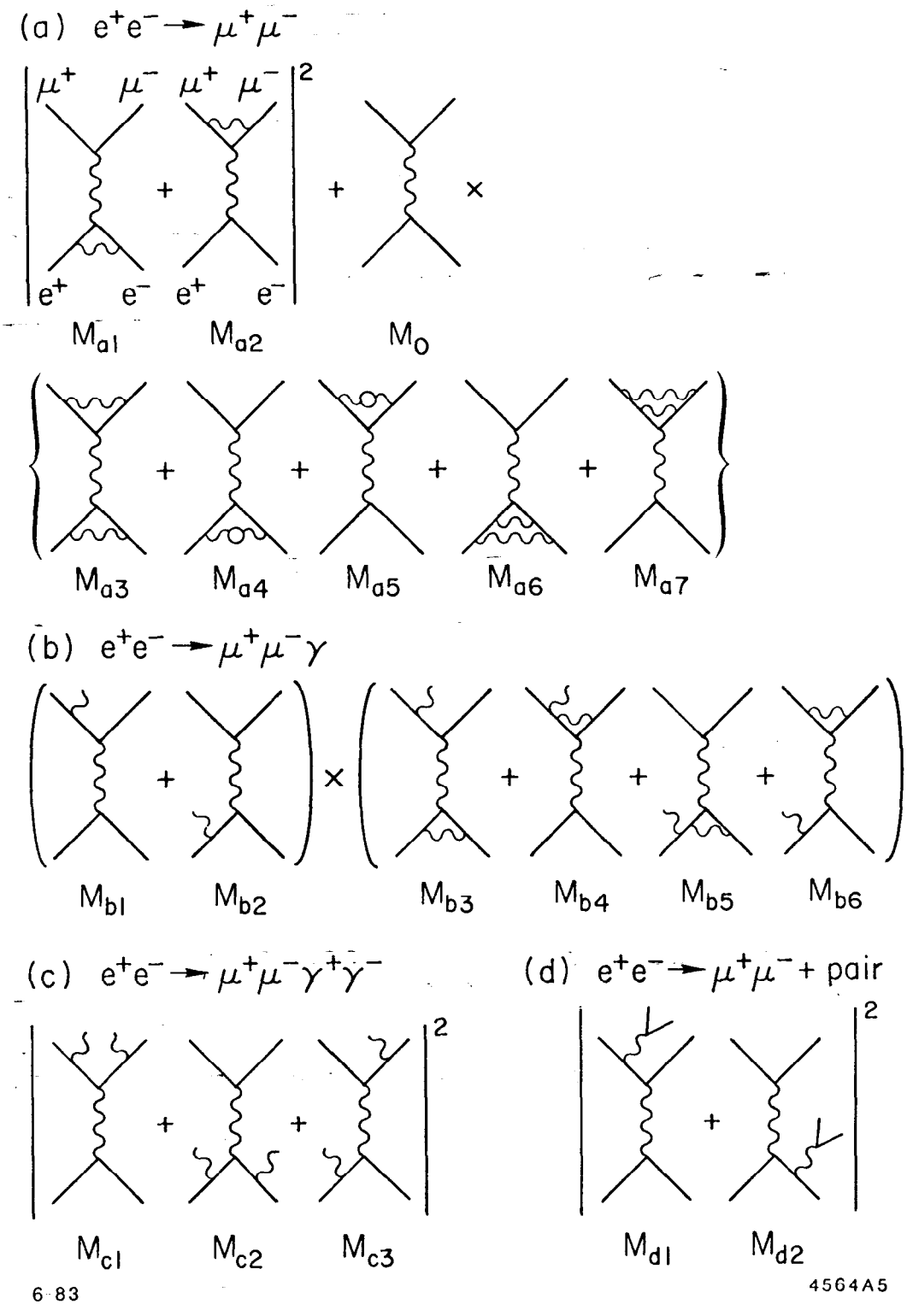
(a) $e^+e^- \to \mu^+\mu^-$
μ^+ μ^- μ^+ μ^-
e^+ e^- e^+ e^-
2
+
+
×
M_{a1} M_{a2} M_0
+ + + +
M_{a3} M_{a4} M_{a5} M_{a6} M_{a7}
(b) $e^+e^- \to \mu^+\mu^-\gamma$
+ × + + +
M_{b1} M_{b2} M_{b3} M_{b4} M_{b5} M_{b6}
(c) $e^+e^- \to \mu^+\mu^-\gamma^+\gamma^-$
+ +
2
M_{c1} M_{c2} M_{c3}
(d) $e^+e^- \to \mu^+\mu^-$ + pair
+
2
M_{d1} M_{d2}
6-83
4564A5

Fig. 5

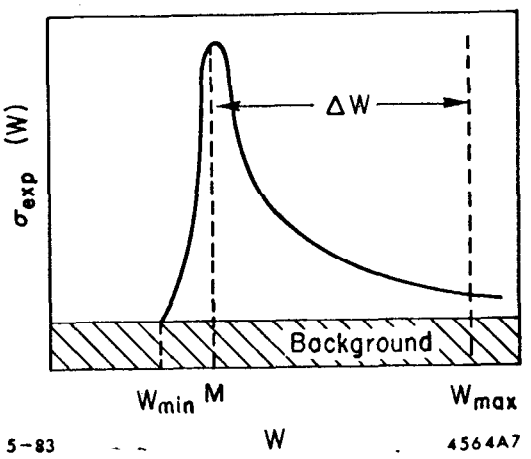

Fig. 6

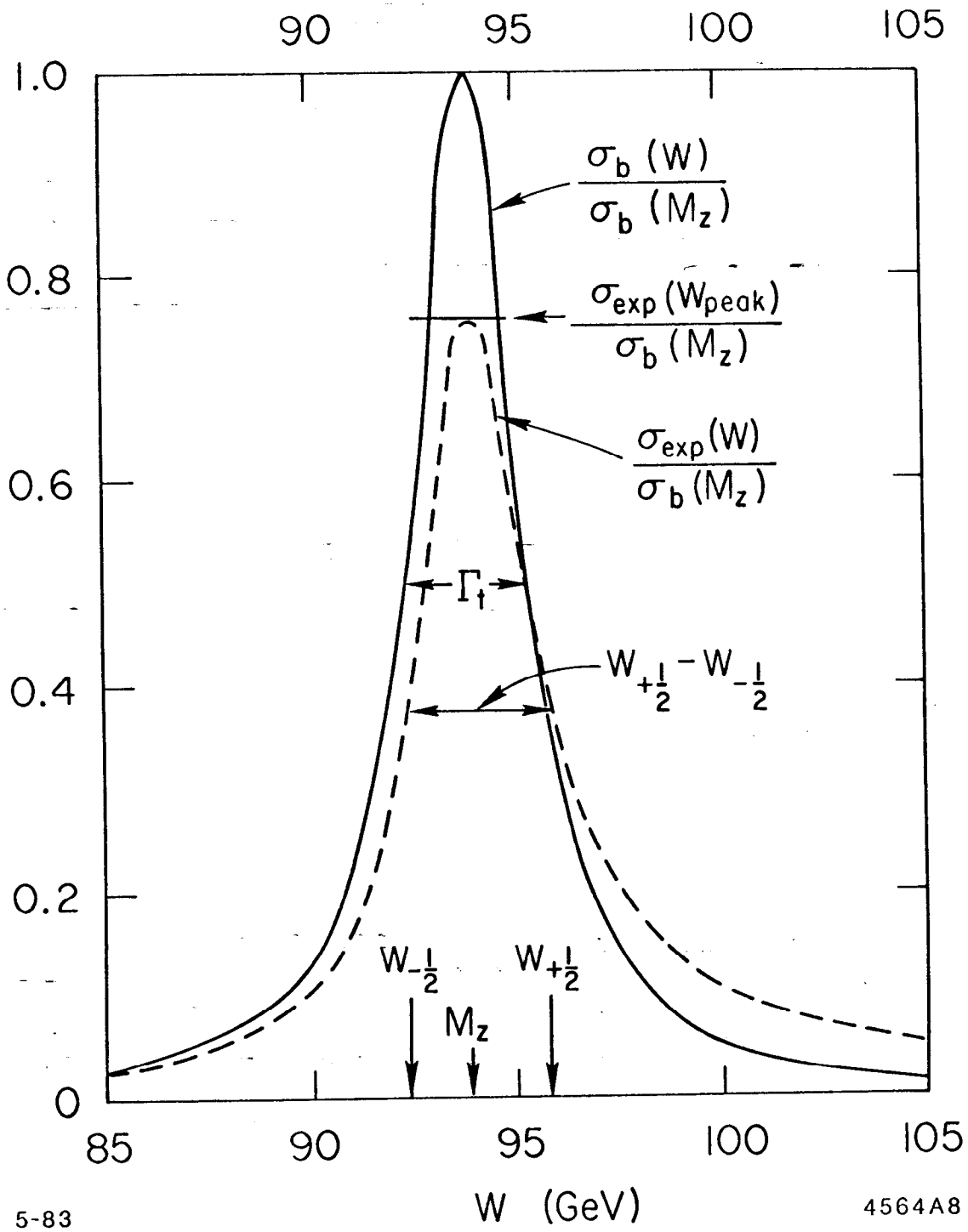
90
95
100
105
1.0
0.8
0.6
0.4
0.2
0
$\frac{\sigma_b(W)}{\sigma_b(M_z)}$
$\frac{\sigma_{exp}(W_{peak})}{\sigma_b(M_z)}$
$\frac{\sigma_{exp}(W)}{\sigma_b(M_z)}$
Γ_t
$W_{+\frac{1}{2}} - W_{-\frac{1}{2}}$
$W_{-\frac{1}{2}}$
$W_{+\frac{1}{2}}$
M_z
85
90
95
100
105
W (GeV)
5-83
4564A8

Fig. 7